Before we start some exciting results...

Last time we saw that the images rotates in a microlensing event
But he image separation is very small a few milli-arcsec
So we don't see it...Except that now with high resolution interferometry
we see the image rotation

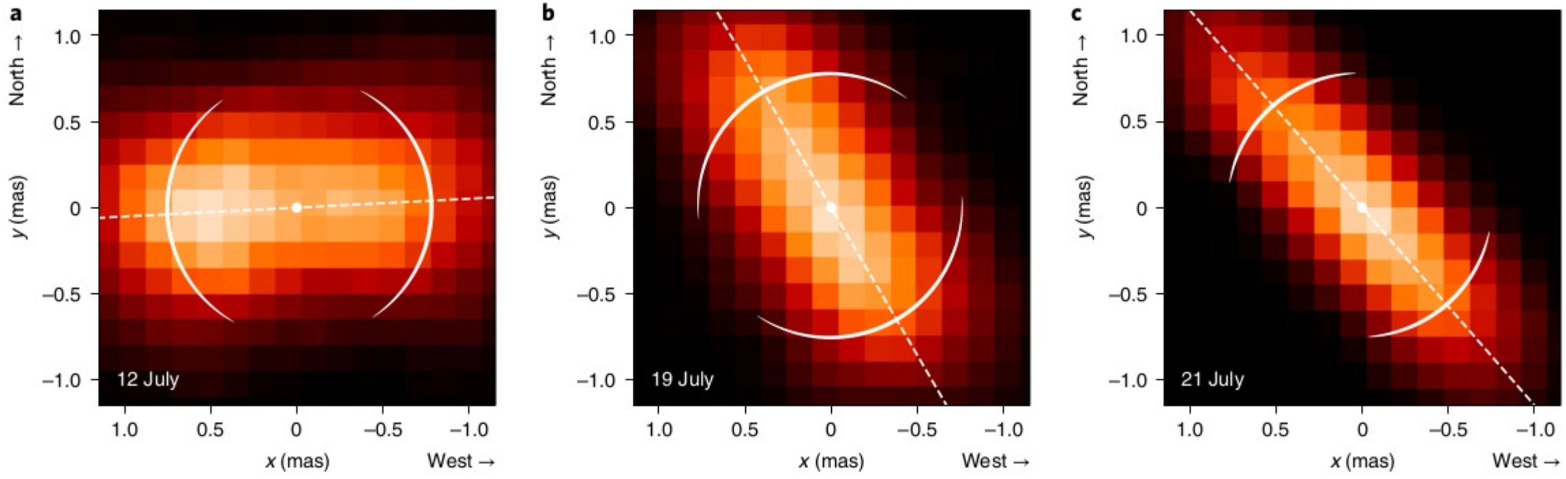

Model free reconstruction from interferometric data
Cassan etal. (2021)

The microlensing Experiments

Basic set-up

Optical depth - rates

Results on dark matter

The case of the galactic bulge

The double lens

Potential – lens equation

Approximate analytical solution

General amplification maps – ray tracing

Some observations and general perspectives

The microlensing projects

Paczynski (1986)

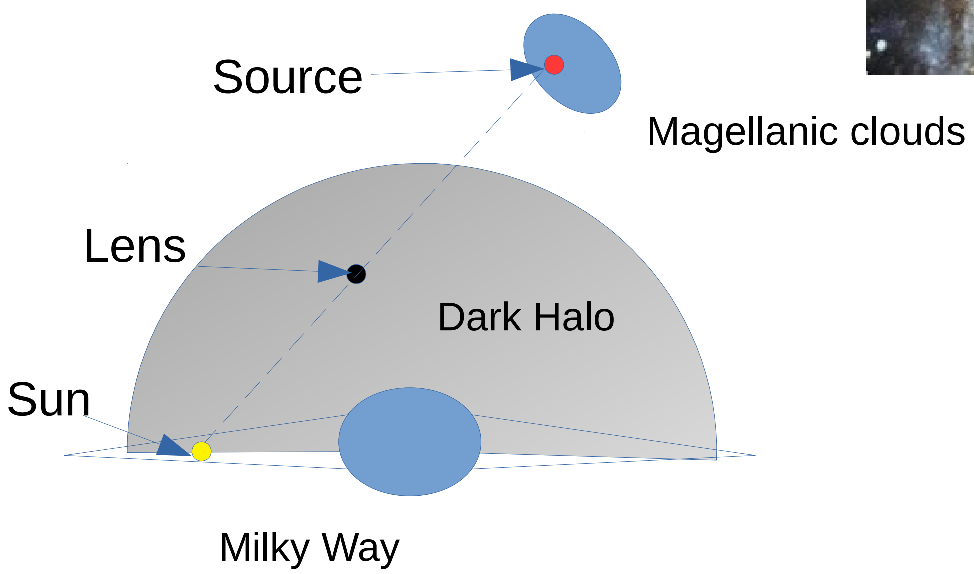

Typical situation a star in the Magellanic cloud is amplified by a lens (dark object) in the galactic halo

The microlensing projects: control situation

Paczynski (1986)

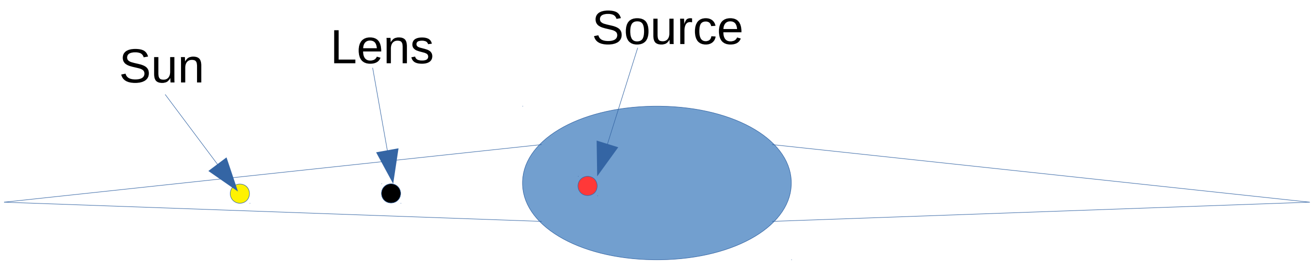

Typical situation a star in the galactic bulge is amplified by a lens (star) in the galactic disk

Observation of a microlensing event in the small Magellanic cloud (EROS project)

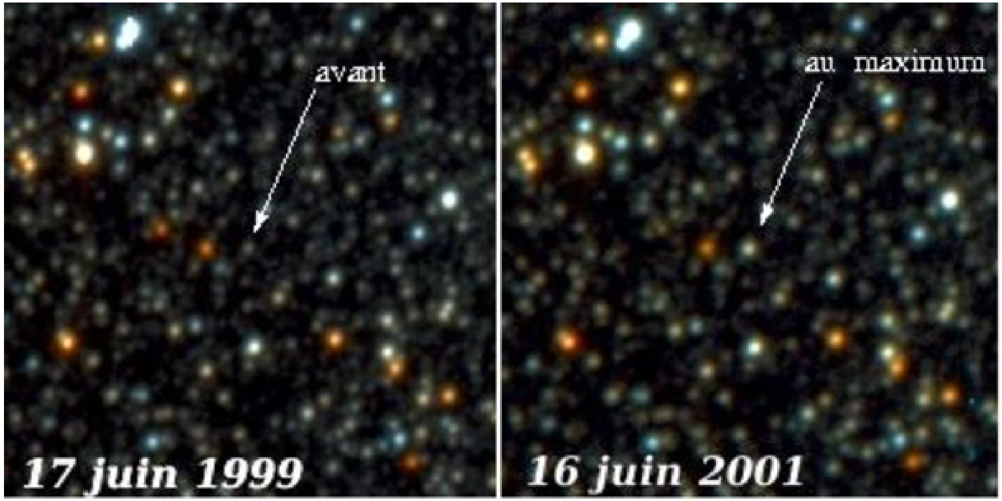

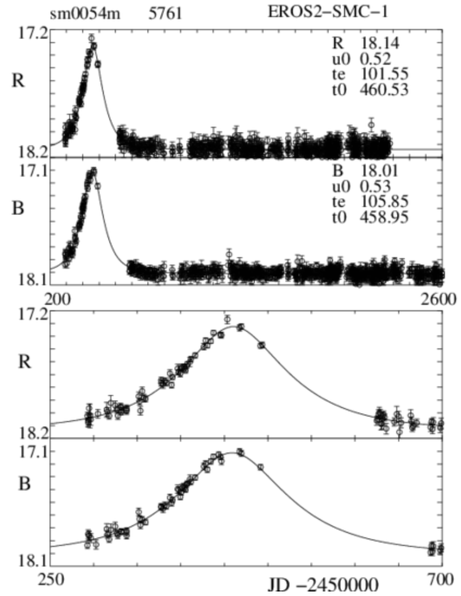

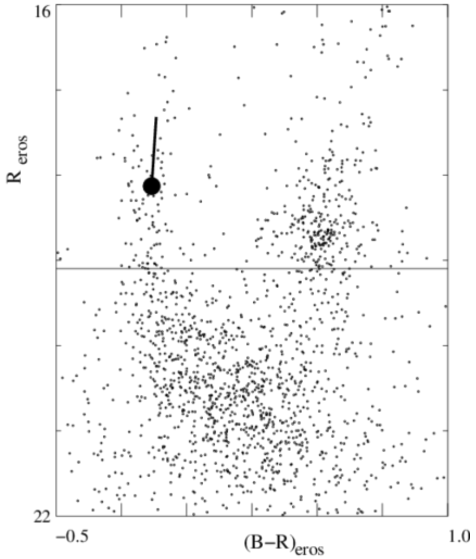

Typical numbers for a microlensing event: $R_E \simeq 1\,UA \quad ; \quad T_E \simeq 30\,days$

The microlensing collaborations

EROS (Milky Way, LMC, SMC)

OGLE (Milky Way)

AGAPE (Andromeda galaxy)

DUO (Milky Way)

MOA collaboration (Milky Way, planets)

Planet (specific alert system)

Optical depth (probability of a microlensing amplification)

The probability of amplification at a given time is the surface covered by the Einstein ring normalized by the total surface covered by the experiment

probability that the source is within an Einstein ring

(angular Einstein ring)

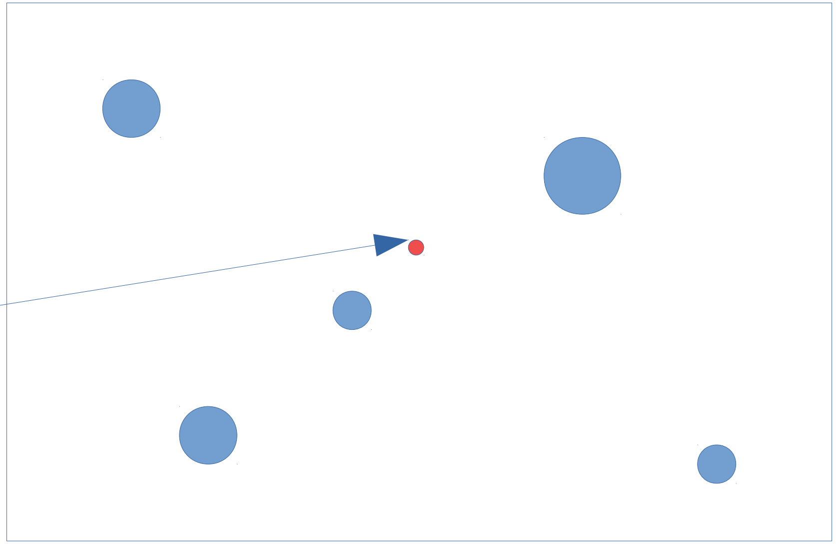

Optical depth

$$\tau = \frac{1}{\Omega} \int \rho_L(D_L) R_E(D_L) D_L^2 \, dD_L$$

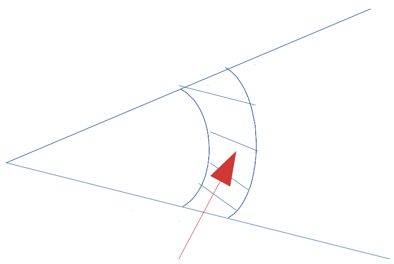

$\rho_L(D_L) D_L^2 \, dD_L$

Approximation: $R_E \simeq C^{ste}$ $\longrightarrow$ $\tau \simeq \frac{R_E^2}{\Omega} N_L \simeq 10^{-6}$

Typical Milky Way
self lensing
(less towards LMC/SMC

For a few millions sources one should see a few amplifications: project should work...

Lensing rates
(number of events per unit time)

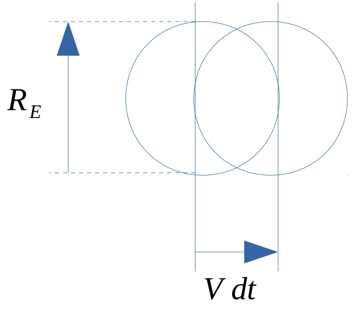

Surface covered per unit time: $R_E V$

$$\Gamma = \frac{1}{\Omega} \int \rho_L(D_l)\, R_E V_t D_L^2 dD_L \simeq \frac{\tau}{T_E}$$

For a total observing time $T_0 \simeq 1\ year$ $\quad N(T_0) = \frac{T_0}{T_E}\ \tau \qquad \tau \simeq 10^{-6} \quad ; \quad T_E \simeq 30\ \ days$

And observing a few millions sources in the Galaxy, a few 10's of events per year

If dark matter is made of compact objects, we should observe also tens of events
Towards the LMC and SMC

The problem has been simplified

Real rates and optical depth involves an integral over the source distribution

$$\tau = \frac{1}{\Omega} \int \int \rho_L(D_L) \rho_S(D_S) R_E(D_L, D_S) D_L^2 \, dD_L \, D_S^2 \, dD_S$$

The integral has to be averaged over the source distribution

Problems with microlensing estimates

The fields are very dense: blending of the source is an issue

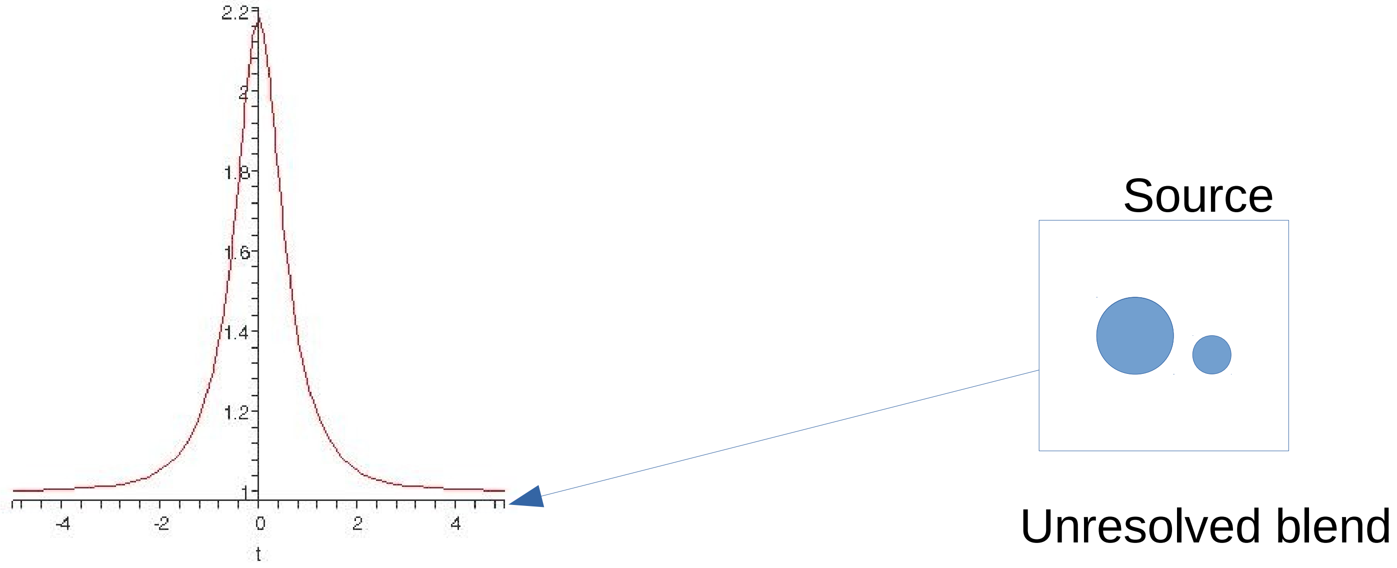

The baseline flux is unknown and over-estimated

The normalization by the baseline flux is degenerate in the fits of the parameters

Over-estimating the baseline flux leads to underestimating T_E and R_E

This requires systematic Monte-Carlo simulations to evaluate the effect of the blends

Or using a specific method to derive unbiased estimates Alard (2001)

But in practice the solution adopted by the lensing experiments was to use the Bulge red giants

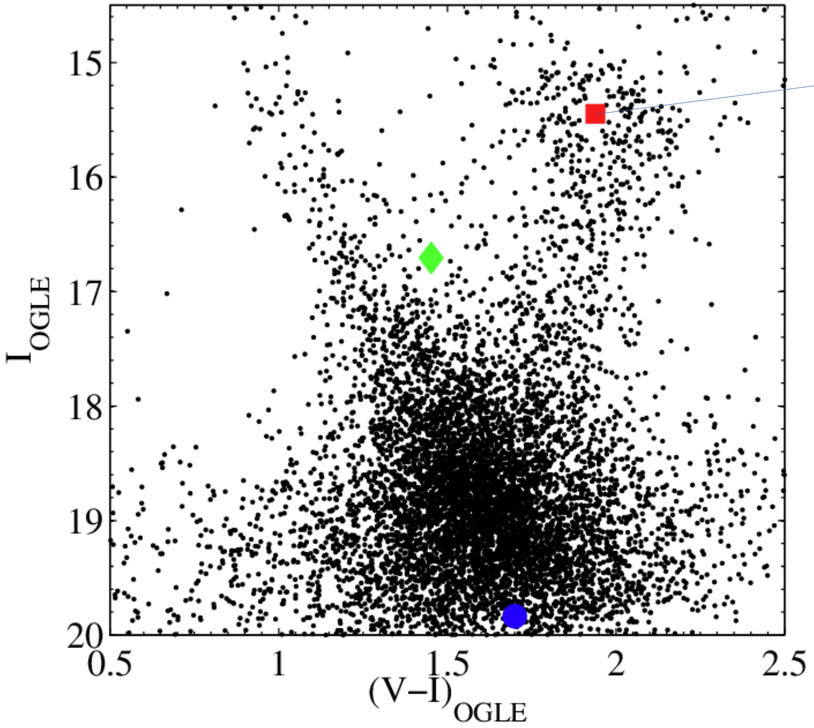

Bright red giants

The red giants are much brighter than the background stars

The effect of blends and associated biases is much smaller

But the problem is not totally gone

The final estimation (Tisserand *etal.* 2007)

From EROS II: an event observed, 39 expected

machos in the mass range $0.6 \times 10-7\, M_{\odot} < M < 15\, M_{\odot}$ are ruled out

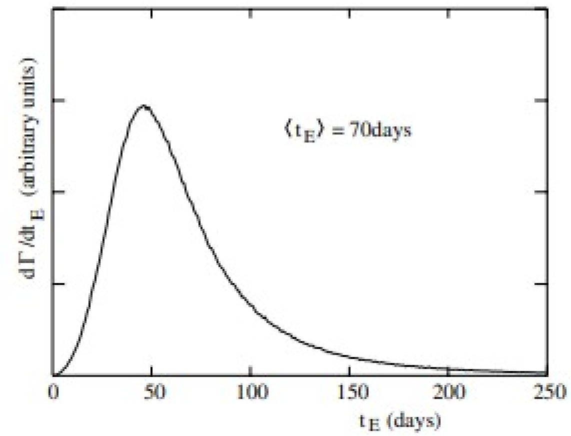

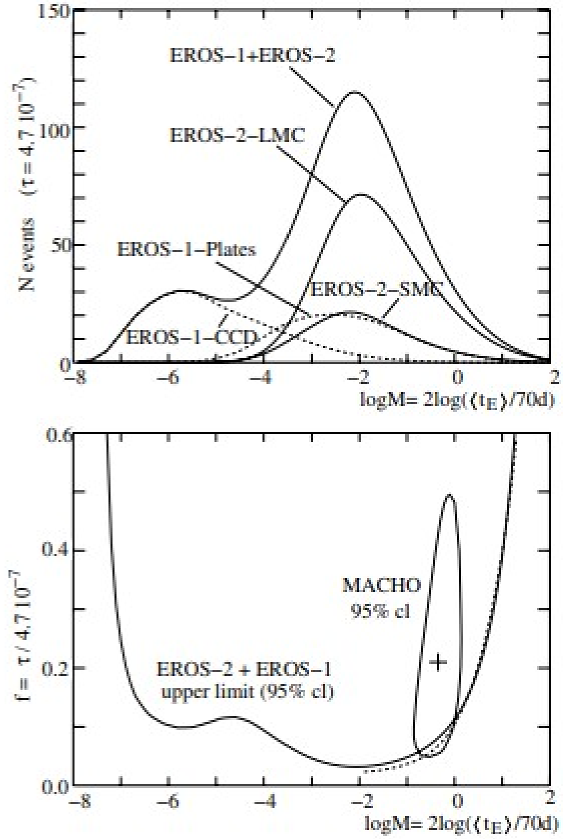

But the experiment towards the center of the Galaxy is very promising...

We find so many microlensing events

And we even start to find some special ones...

A double lens

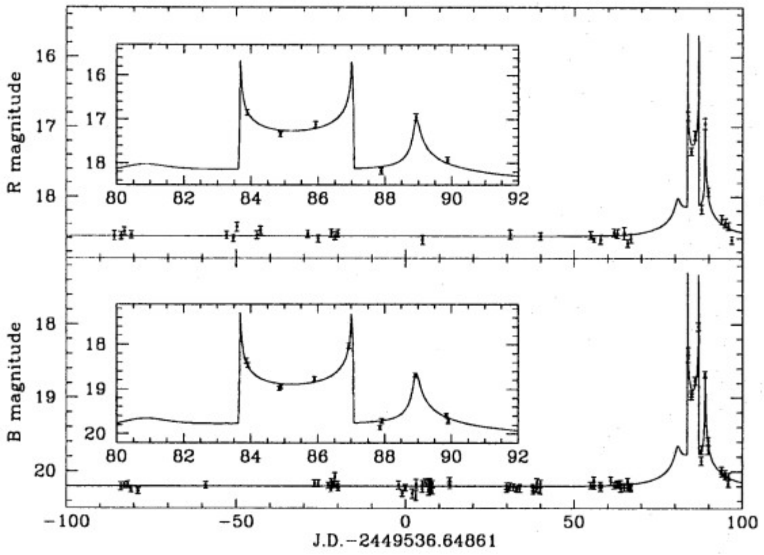

DUO 2

A first case showing finite source size effect

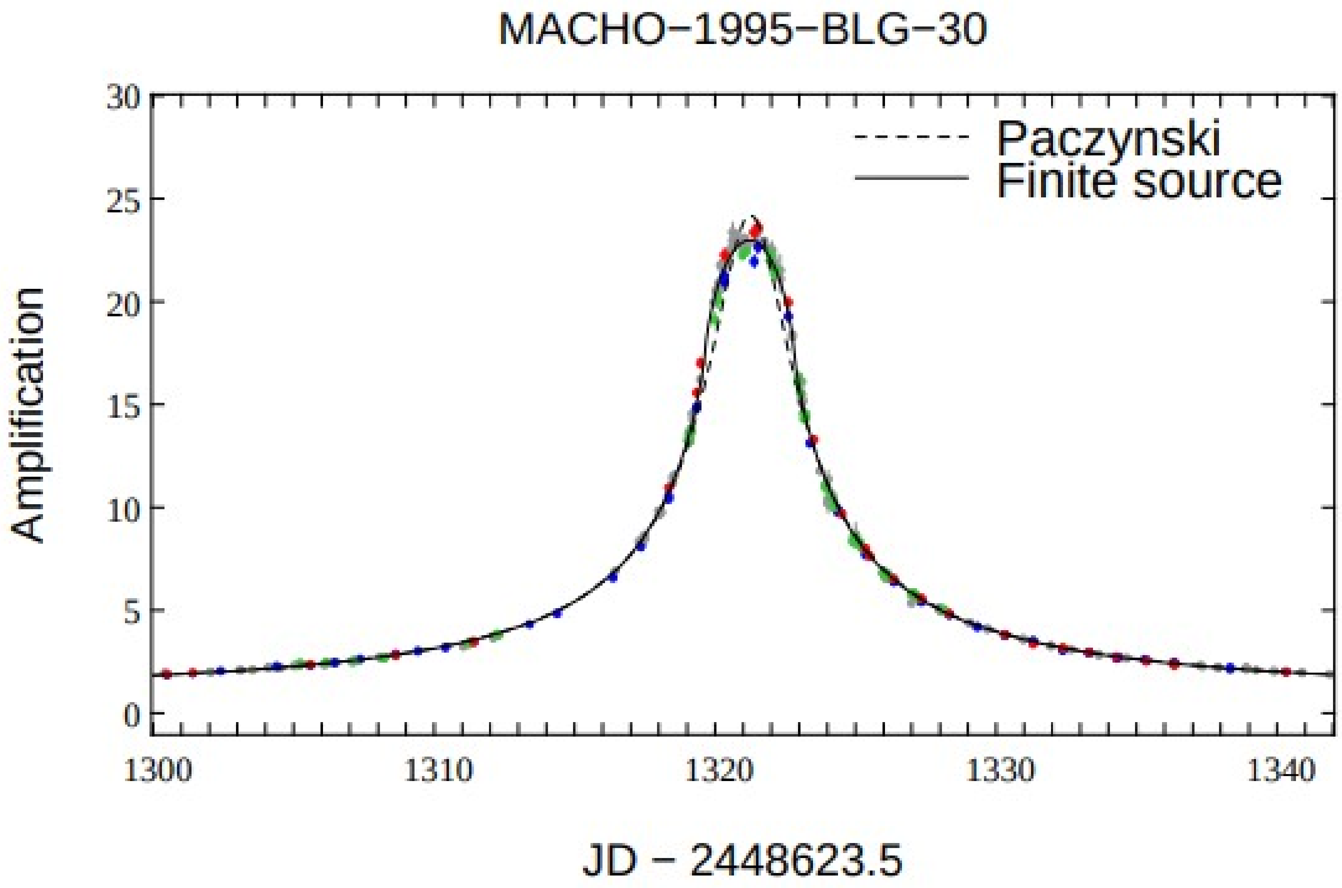

What is really going on with microlensing experiments towards the galactic bulge?
Why so many events ??

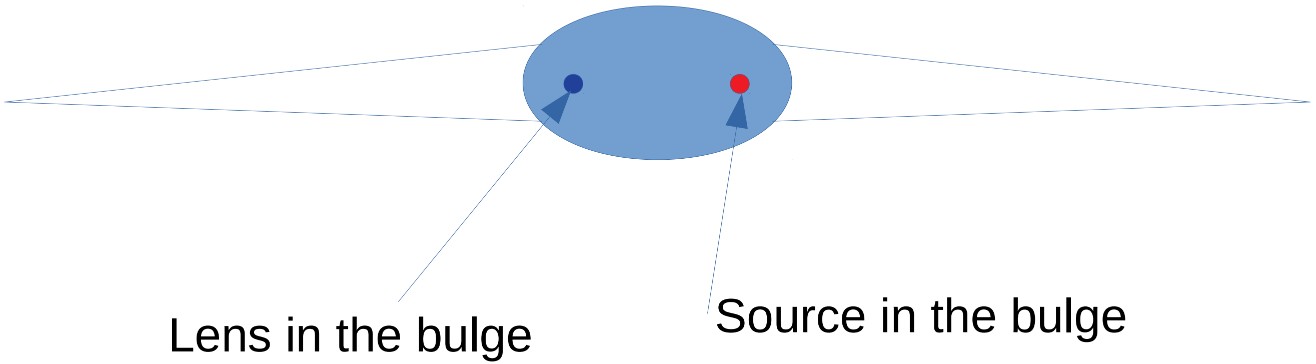

Self-lensing in the Galactic Bulge is very efficient

The probability of amplification of a Bulge star by a Bulge star is larger than the probability of amplification of a Bulge source by a disk lens

Kiraga & Paczynski (1994)

Consequence: a lot of events towards the galactic Bulge

Typical optical depth Bulge-Bulge $\tau \simeq 2 \times 10^{-6}$

Typical optical depth Bulge-Disk $\tau \simeq 0.5 \times 10^{-6}$

Why is it so efficient ?

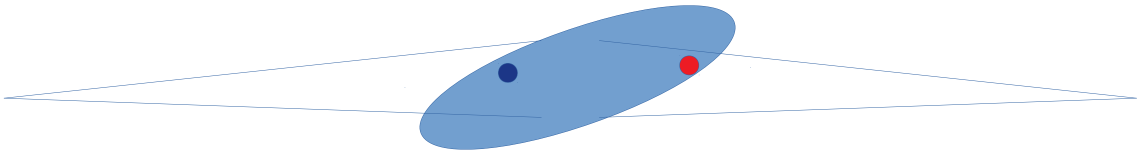

Our galaxy has a central bar: the bulge is quite elongated
The effect is to increase distances, the Einstein radius, and the optical depth

Microlensing with a two point mass lens

Description of the problem

General equations

Approximate analytical solution

Ray tracing

Caustics reconstruction

Specific cases

Global results

Some interesting illustrations

For convenience we use lens plane coordinates: $\vec{r}_S = \vec{\beta} D_L \quad \vec{r} = \vec{\theta} D_L$

$$\phi(\vec{r}) = \frac{1}{\pi} \int_{LP} \kappa(\vec{r}_i) \log\left(|\vec{r} - \vec{r}_i|\right) d^2 r_i \qquad \vec{\alpha}_L(\vec{r}) = D_L \vec{\nabla} \phi(\vec{r})$$

$$\vec{r}_S = \vec{r} - \vec{\alpha}_L \longrightarrow \vec{r}_S = \vec{r} - \vec{\nabla} \phi$$

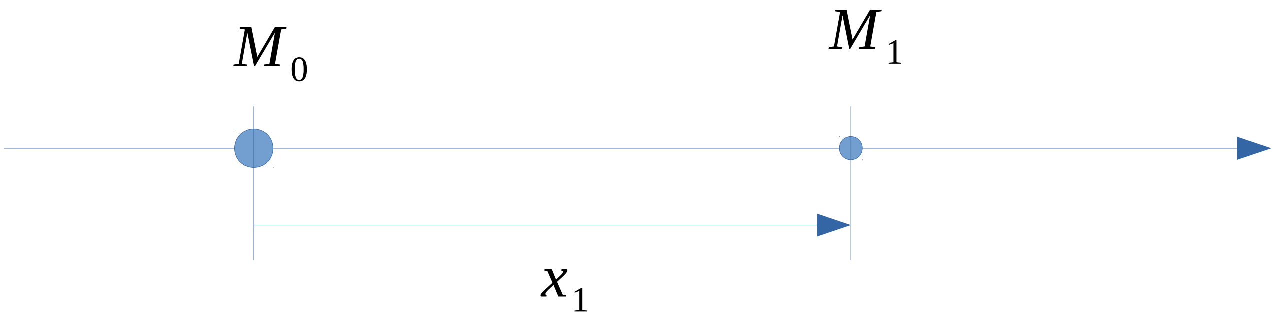

$$\Sigma \equiv M\,\delta(x)\,\delta(y) \quad \rightarrow \quad \int \Sigma\, dx\, dy = M$$

Here: $$\kappa = \frac{\Sigma}{\Sigma_{cr}} = \frac{1}{\Sigma_{cr}}\left(M_0\,\delta(x)\,\delta(y) + M_1\,\delta(x - x_1)\,\delta(y)\right)$$

$$\Sigma_{cr} = \frac{c^2 D_S}{4\pi G D_{LS} D_L}$$

$$R_E^2 = \frac{4GM}{c^2} \frac{D_{LS} D_L}{D_S}$$

$$\frac{M_I}{\Sigma_{cr}} = \frac{4\pi G D_{LS} D_L M}{c^2 D_S} = \pi R_{E,i}^2$$

$$\kappa = \frac{1}{\Sigma_{cr}} \left(M_0 \delta(x) \delta(y) + M_1 \delta(x - x_1) \delta(y) \right) = \pi \left(R_{E,0}^2 \delta(x) \delta(y) + R_{E,1}^2 \delta(x - x_1) \delta(y) \right)$$

$$\phi(\vec{r}) = \frac{1}{\pi} \int_{LP} \kappa(\vec{r}_i) \log\left(|\vec{r} - \vec{r}_i| \right) d^2 r_i = R_{E,0}^2 \log(r) + \frac{R_{E,1}^2}{2} \log\left((x - x_1)^2 + y^2 \right)$$

The lens equation: $\vec{r}_s = \vec{r} - \vec{\nabla}\phi$ Is re-normalized

We renormalized the lens equation by: $R_{E,0}$ $\longrightarrow$ $\vec{r}_S \equiv \dfrac{r_S}{R_{E,0}}$; $\vec{r} \equiv \dfrac{r}{R_{E,0}}$

v

$\longrightarrow$ $\phi \equiv \dfrac{\phi}{R_{E,0}^2}$ (note the gradient introduce an additional normalization for ϕ)

$$\phi(\vec{r}) = R_{E,0}^2 \log(r) + \frac{R_{E,1}^2}{2} \log\left((x-x_1)^2 + y^2\right)$$

$\downarrow$

Renormalized potential

$$\phi(\vec{r}) = \log(r) + \frac{\mu}{2} \log\left((x-x_1)^2 + y^2\right)$$

With: $\mu = \dfrac{R_{E,1}^2}{R_{E,0}^2} = \dfrac{M_1}{M_0}$

Equations for the images

$$\vec{r}_s = \vec{r} - \vec{\nabla}\phi \longrightarrow \begin{cases} x_s = x - \dfrac{x}{r^2} - \dfrac{\mu(x - x_1)}{(x - x_1)^2 + y^2} \\ y_s = y - \dfrac{y}{r^2} - \dfrac{\mu y}{(x - x_1)^2 + y^2} \end{cases}$$

$$\phi(\vec{r}) = \log(r) + \frac{\mu}{2}\log\left((x - x_1)^2 + y^2\right) \qquad r^2 = x^2 + y^2$$

Reducing each equation to a common denominator leads to 5^{th} order in x and y

Unlike the single point mass lens there is no analytical solution
Relating the image to the source position

However for large enough separation between the 2 components
An expansion of the potential is possible

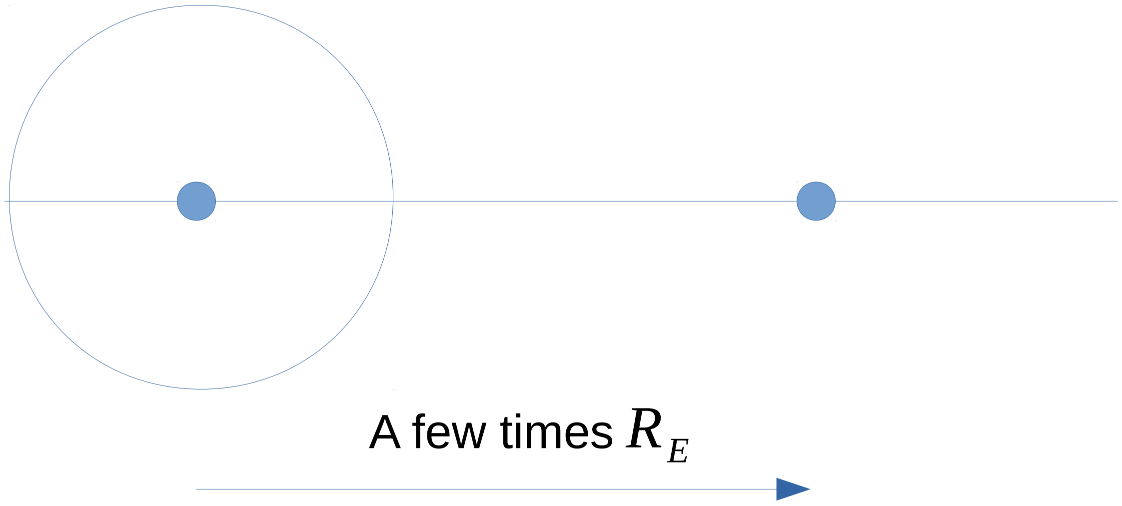

We will study the Jacobian to identify the singularities in amplification

Unlike the single point mass lens
Where a singularity occur at single position
when the source is aligned with the lens

In the 2 points mass lens singularities occur
For an infinity of positions of the source
All those positions are on a system of line: the caustics

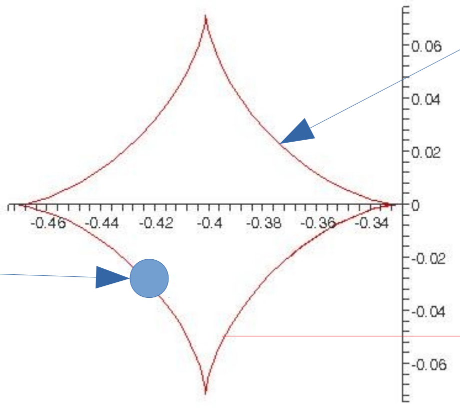

Source position

Caustics lines

Analytical solutions for the critical lines And caustics lines

For large separation between the masses

In contrast to the single point mass lens

When a circle become an ellipsoid
(critical lines)

When a point become a series of lines
(caustics lines)

We will consider that the field of the first (main) component can be linearized locally near the second component

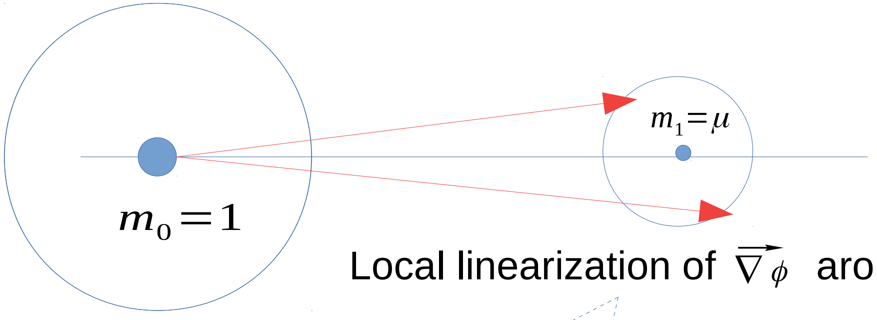

Local linearization of $\vec{\nabla}\phi$ around m_1

$$\phi=\mu\log(r)+\frac{1}{2}\log\left((x+x_1)^2+y^2\right)\simeq\log(x_1)+\mu\log(r)+\frac{x}{x_1}+\frac{y^2-x^2}{2x_1^2}$$

Displacement term

Distortion (shear)

Expansion at order 2 in $\frac{1}{x_1}$

In this approximation the solution for the critical lines and caustics
Is analytical

$$J = \frac{\partial x_s}{\partial x}\frac{\partial y_s}{\partial y} - \frac{\partial x_s}{\partial y}\frac{\partial y_s}{\partial x}$$ with $$\vec{r}_S = \vec{r} - \vec{\nabla}\phi$$

Expansion at order 2 in $\frac{1}{x_1}$

$$J = \frac{r^4 - \mu^2}{r^4} - 2\mu\frac{\cos(2\theta)}{r^2 x_1^2}$$

Critical lines: J=0 $$r = \sqrt{\mu}\left(1 + \cos\frac{(2\theta)}{2x_1^2}\right)$$

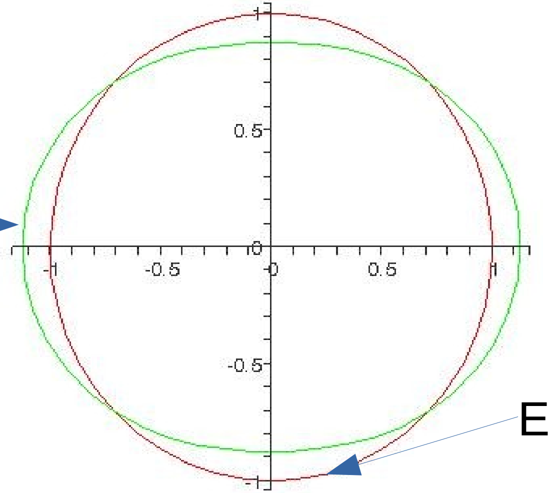

Einstein ring

Caustics: transformation of the critical line in source plane coordinates

Take critical line equation $r=\sqrt{\mu}\left(1+\cos\frac{(2\theta)}{2x_1^2}\right)$

Insert in lens equation

$\vec{r}_S=\vec{r}-\vec{\nabla}\phi$

Expansion at order 2 in $\frac{1}{x_1}$

$$\left\{\begin{aligned} x_S &= -1/x_1+\sqrt{\mu}\,\frac{3\cos(\theta)+\cos(3\theta)}{2x_1^2} \\ y_S &= \sqrt{\mu}\,\frac{-3\sin(\theta)+\sin(3\theta)}{2x_1^2} \end{aligned}\right\}$$

Numerical application: shape of the caustics

$$x_1 = 2.5 \quad ; \quad \mu = 0.05$$

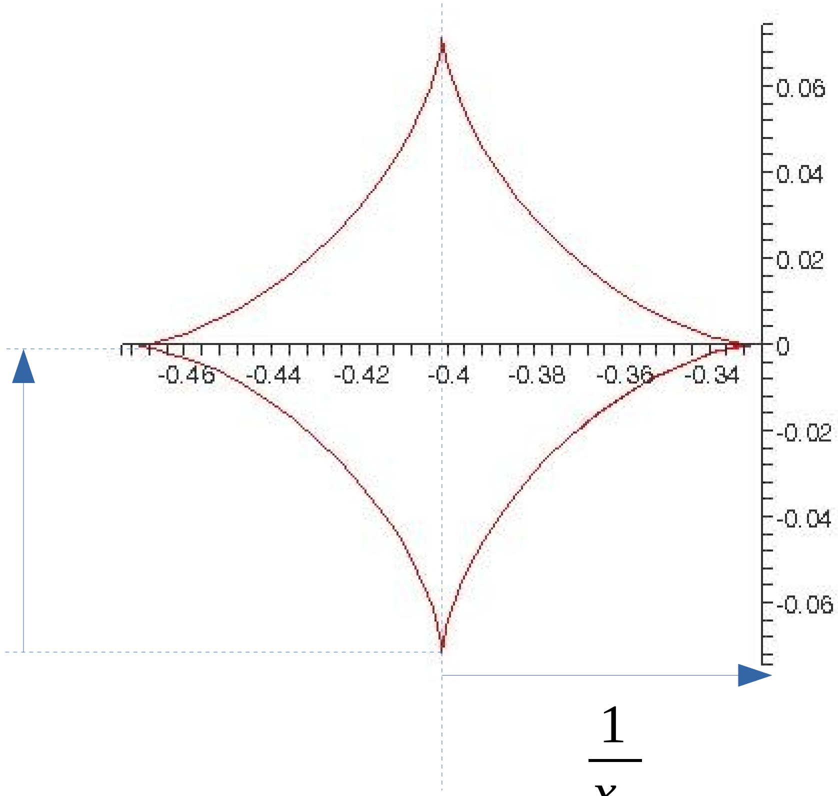

Amplitude $2\frac{\sqrt{\mu}}{x_1^2}$

$\frac{1}{x_1}$

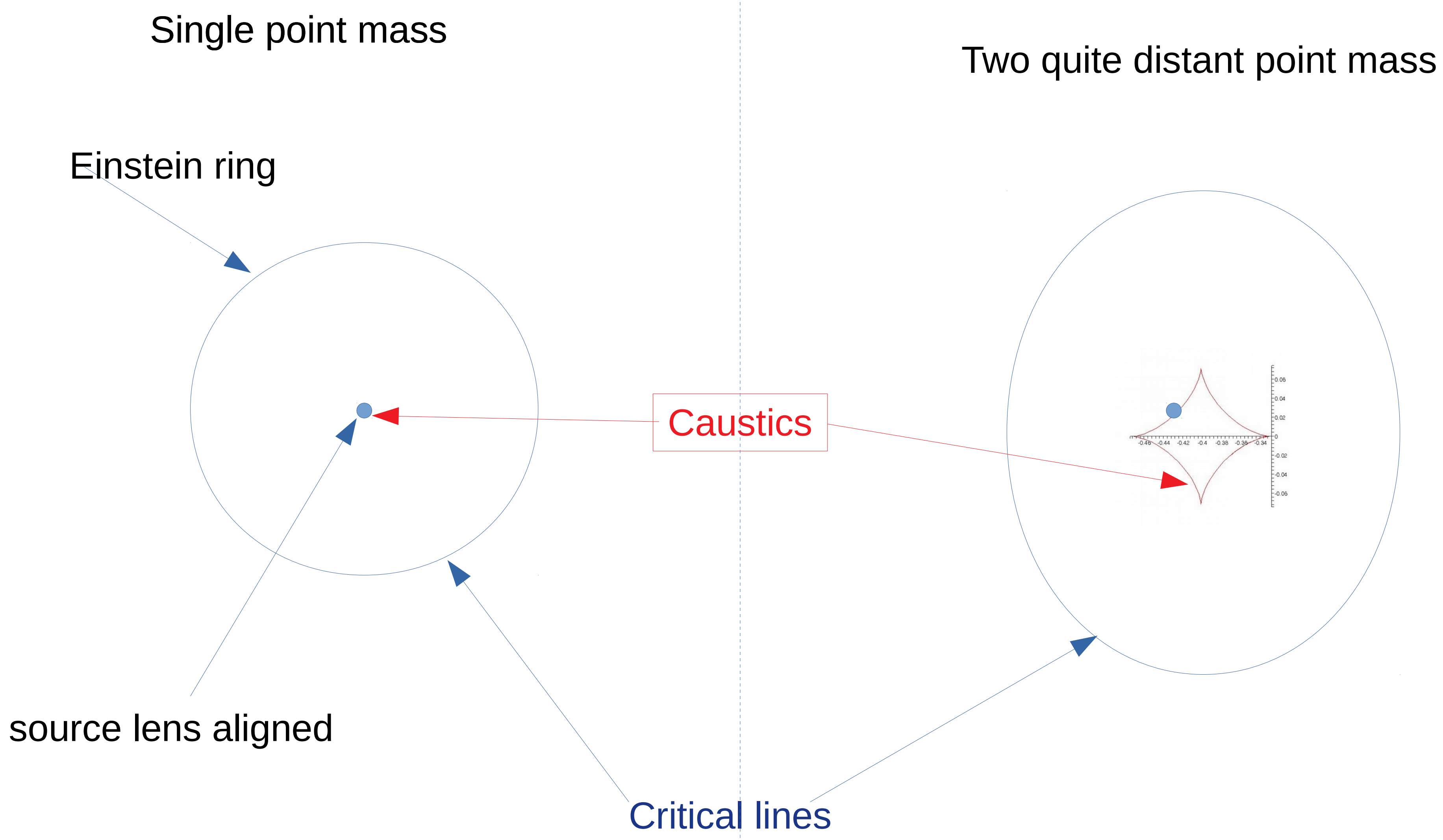
Single point mass
Two quite distant point mass
Einstein ring
Caustics
source lens aligned
Critical lines

Comparison with results from ray tracing

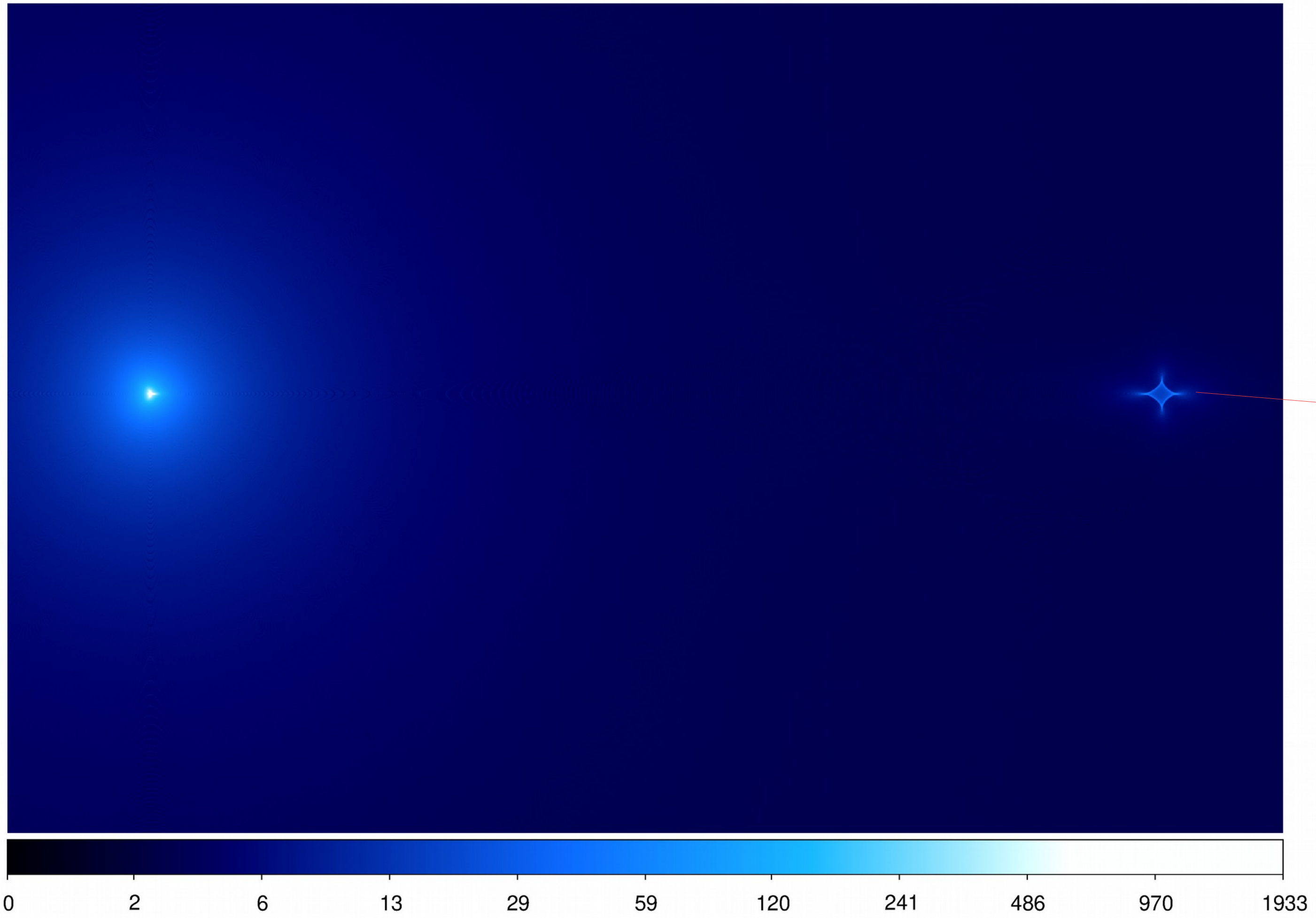

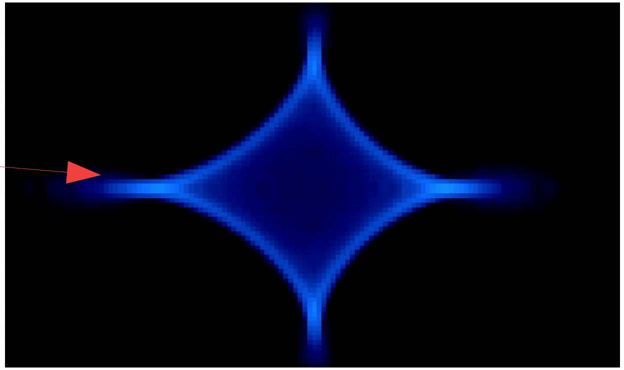

Mass ratio 0.01
Distance 2.5

Distance unit: Einstein radius
Of main component

Single point mass

The ray tracing technique

$$\vec{r}_S = \vec{r} - \vec{\nabla}\phi$$

Several counts in a single source plane bin

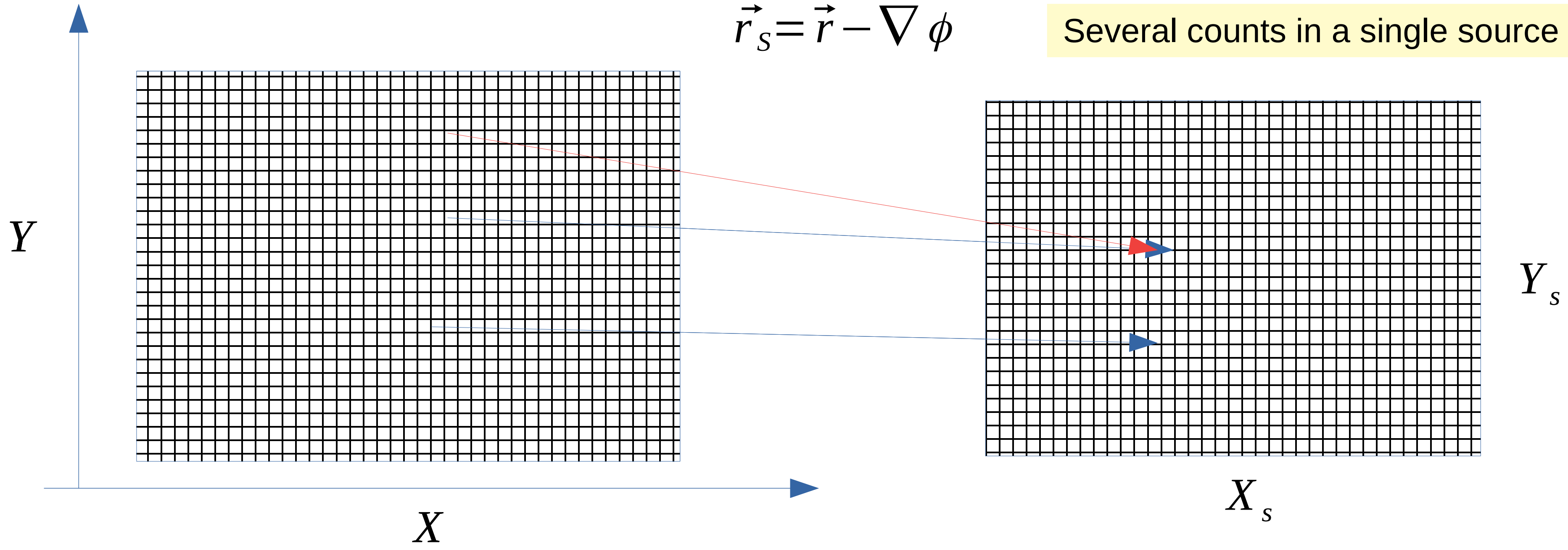

Take a grid in the lens plane: transport to source plane using the lens equation

Estimating the counts in the source plane give the amplification map

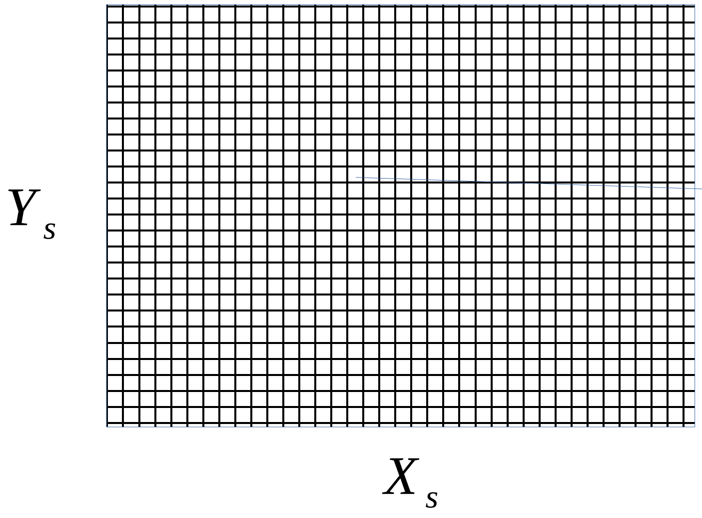

Number counts give the number
Of image (grid points) and thus
The amplification of a source
element

The singularities in the amplification map are the caustics

Ray tracing: reconstructing the images of the source

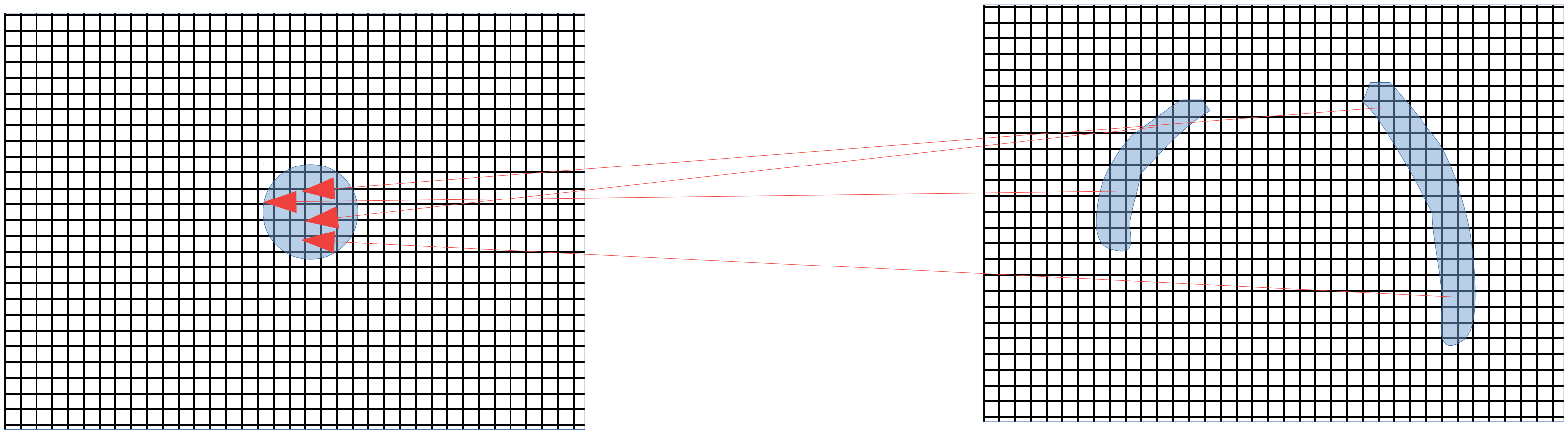

Source plane

Lens plane

All rays from the lens plane going inside the source are the image of the source

Taking the lens closer: some asymmetry develops in the caustic

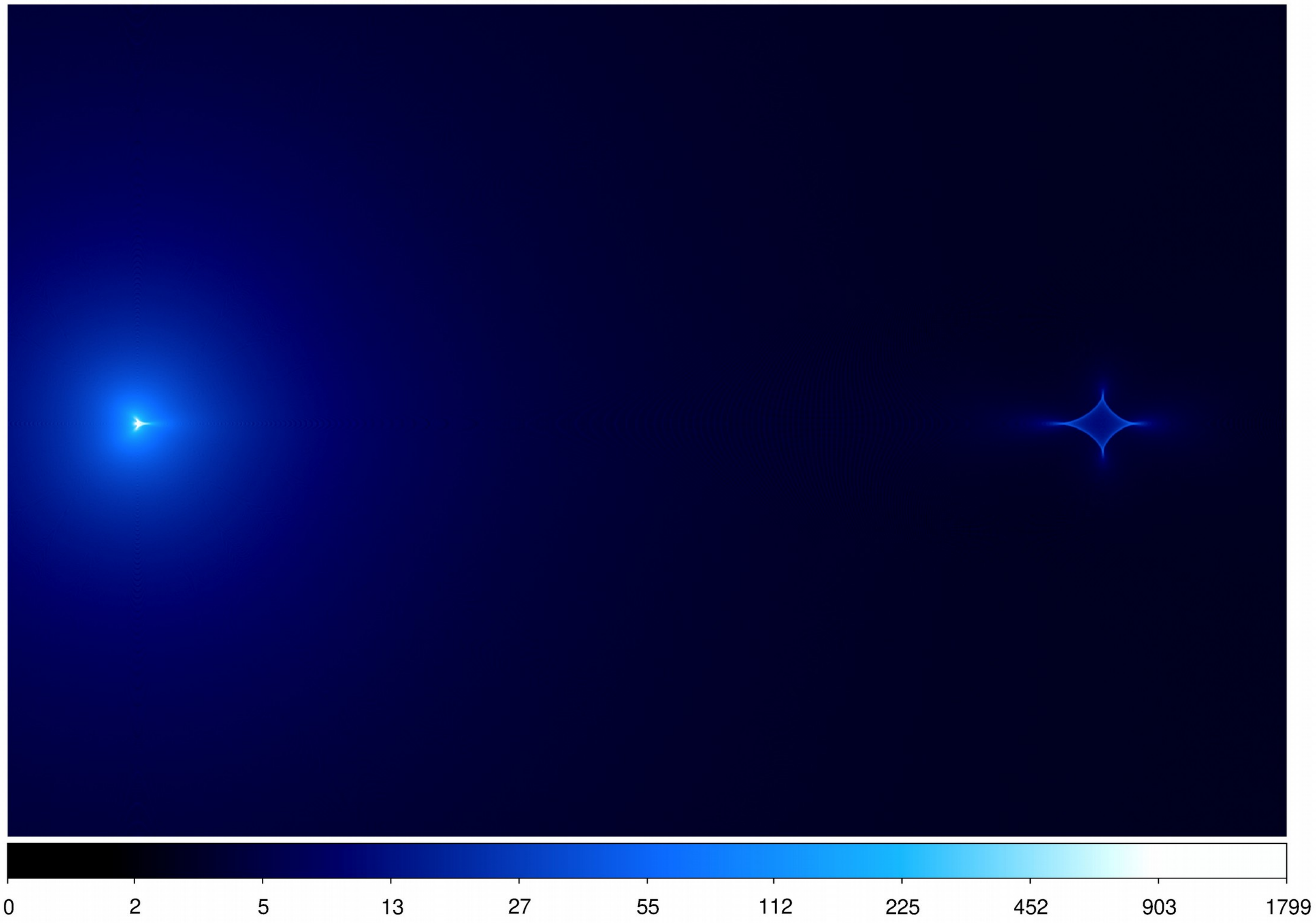

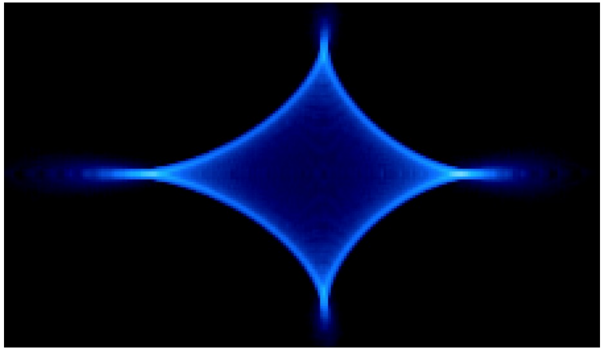

Mass ratio 0.01
Distance 2.0

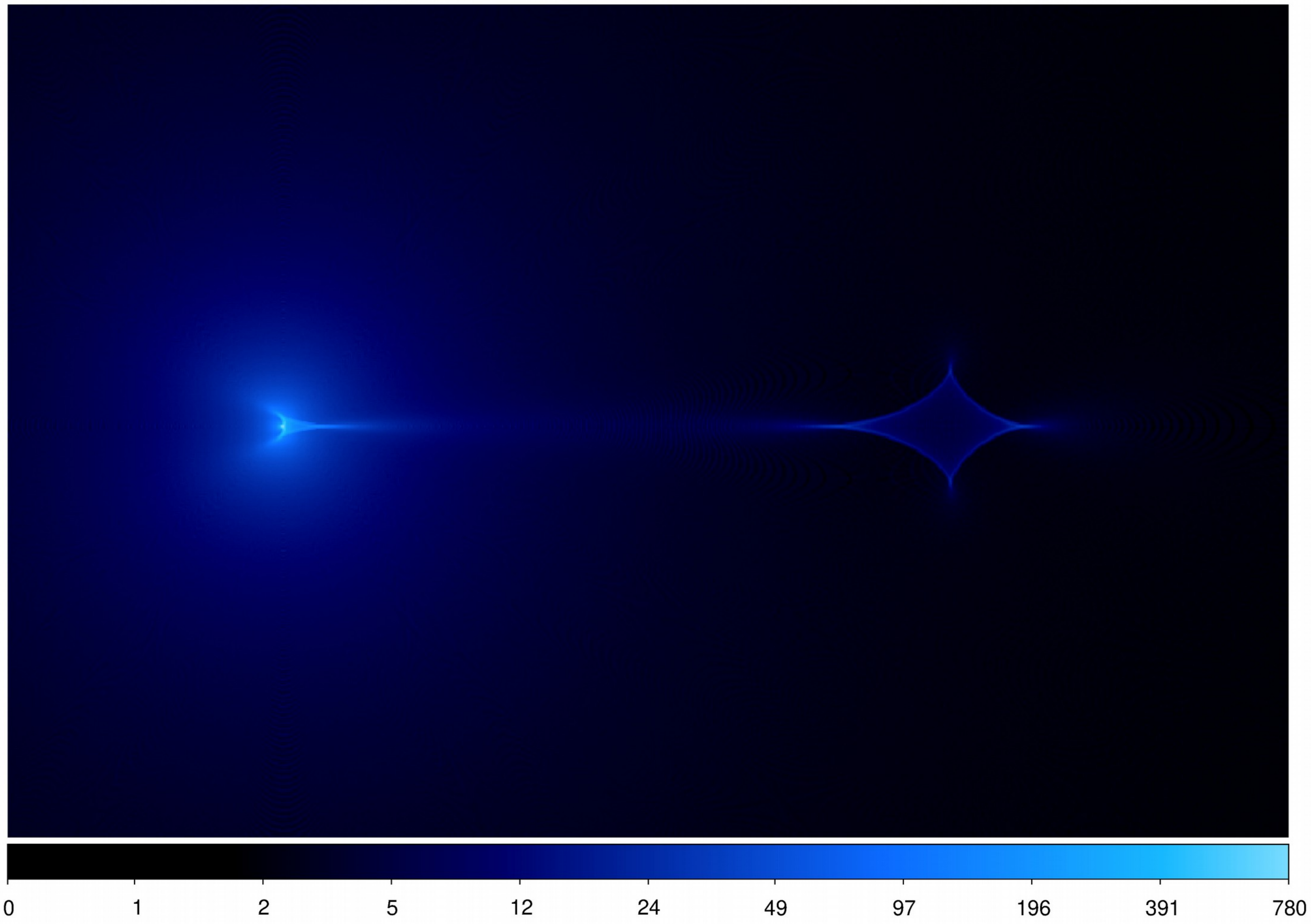

Mass ratio 0.01
Distance 1.5

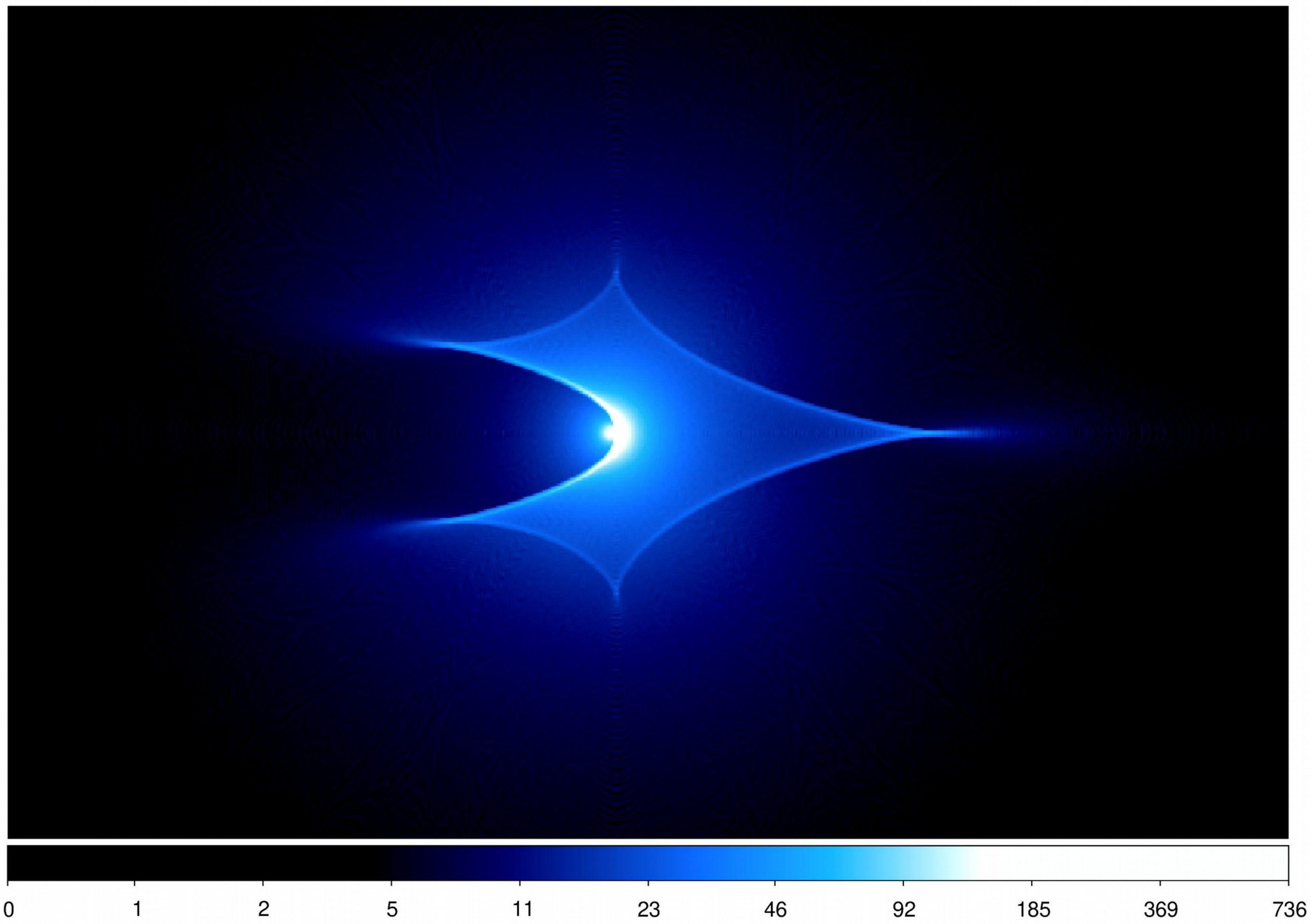

Mass ratio 0.01
Distance 1.0

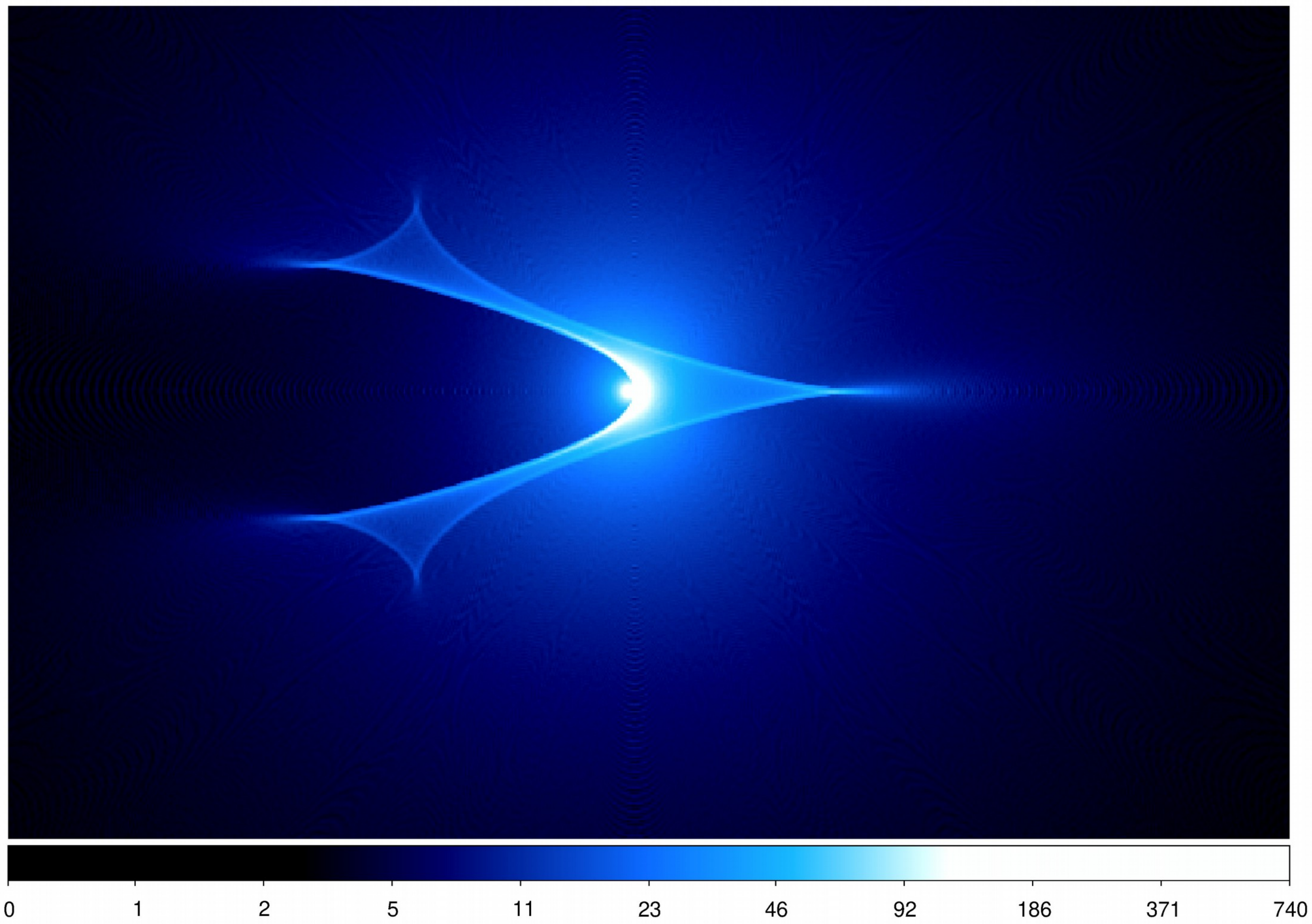

Mass ratio 0.01
Distance 0.9

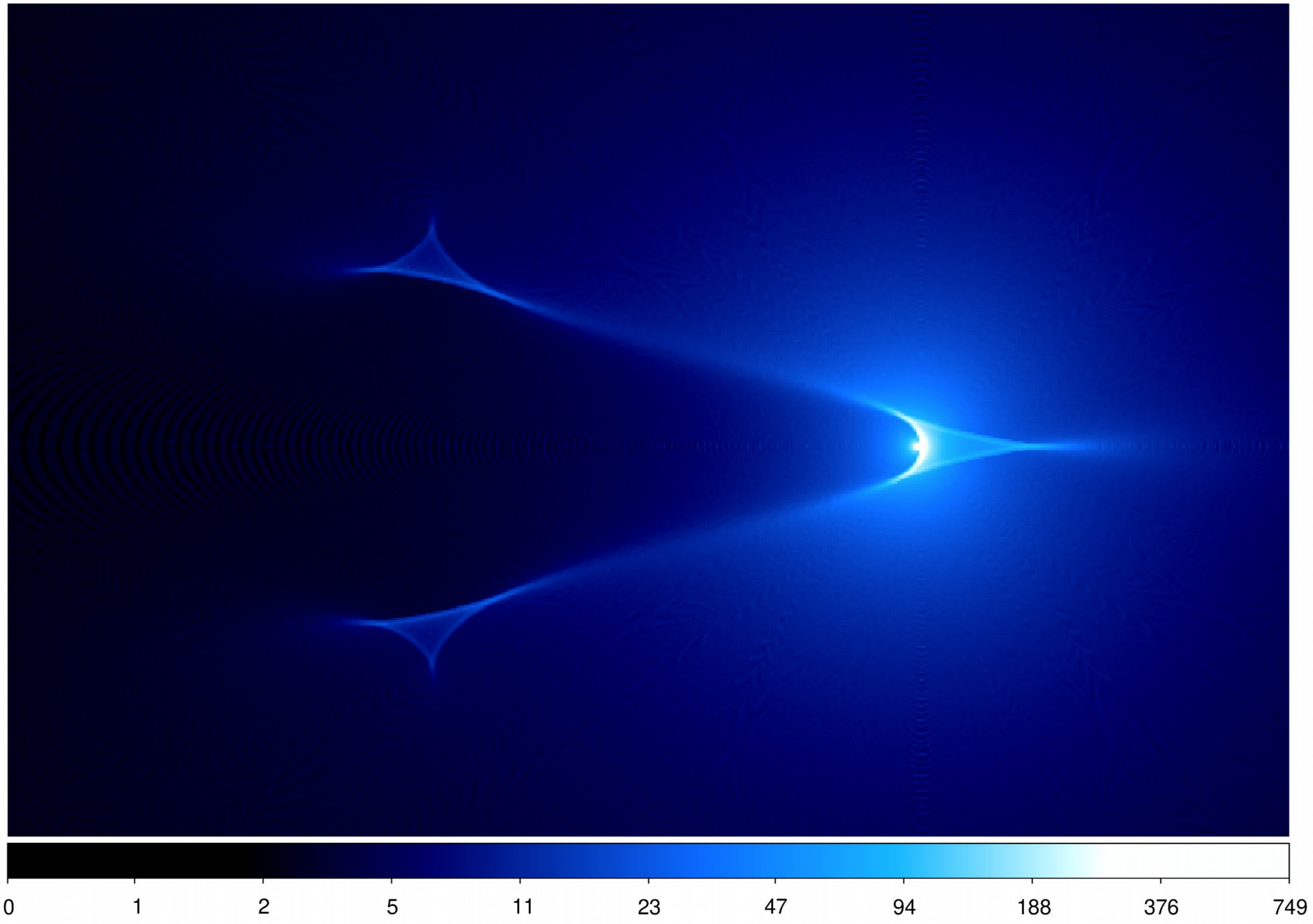

Mass ratio 0.01
Distance 0.8

Caustic merging

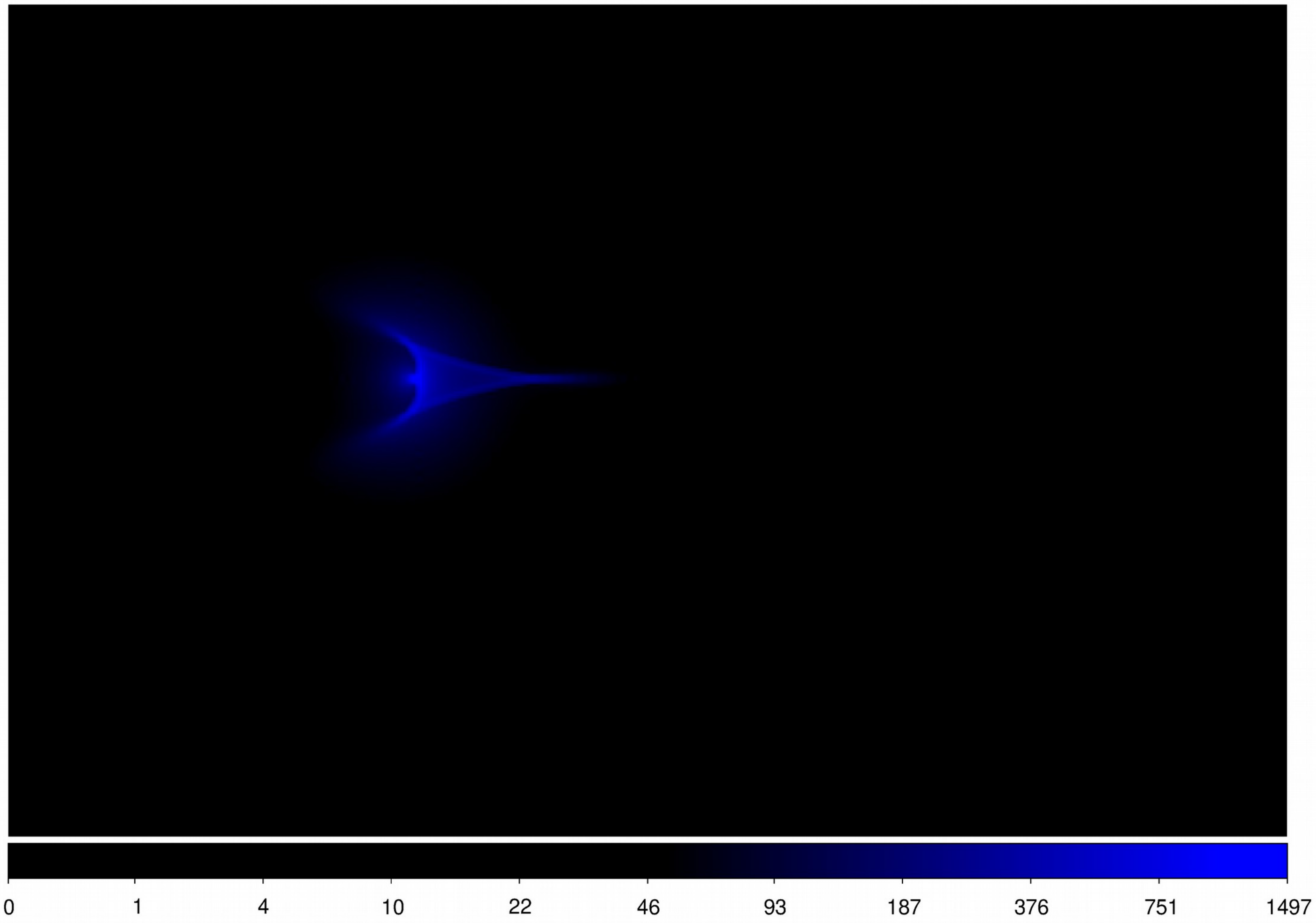

Mass ratio 0.01
Distance 0.7

Consider trajectories in the amplification map

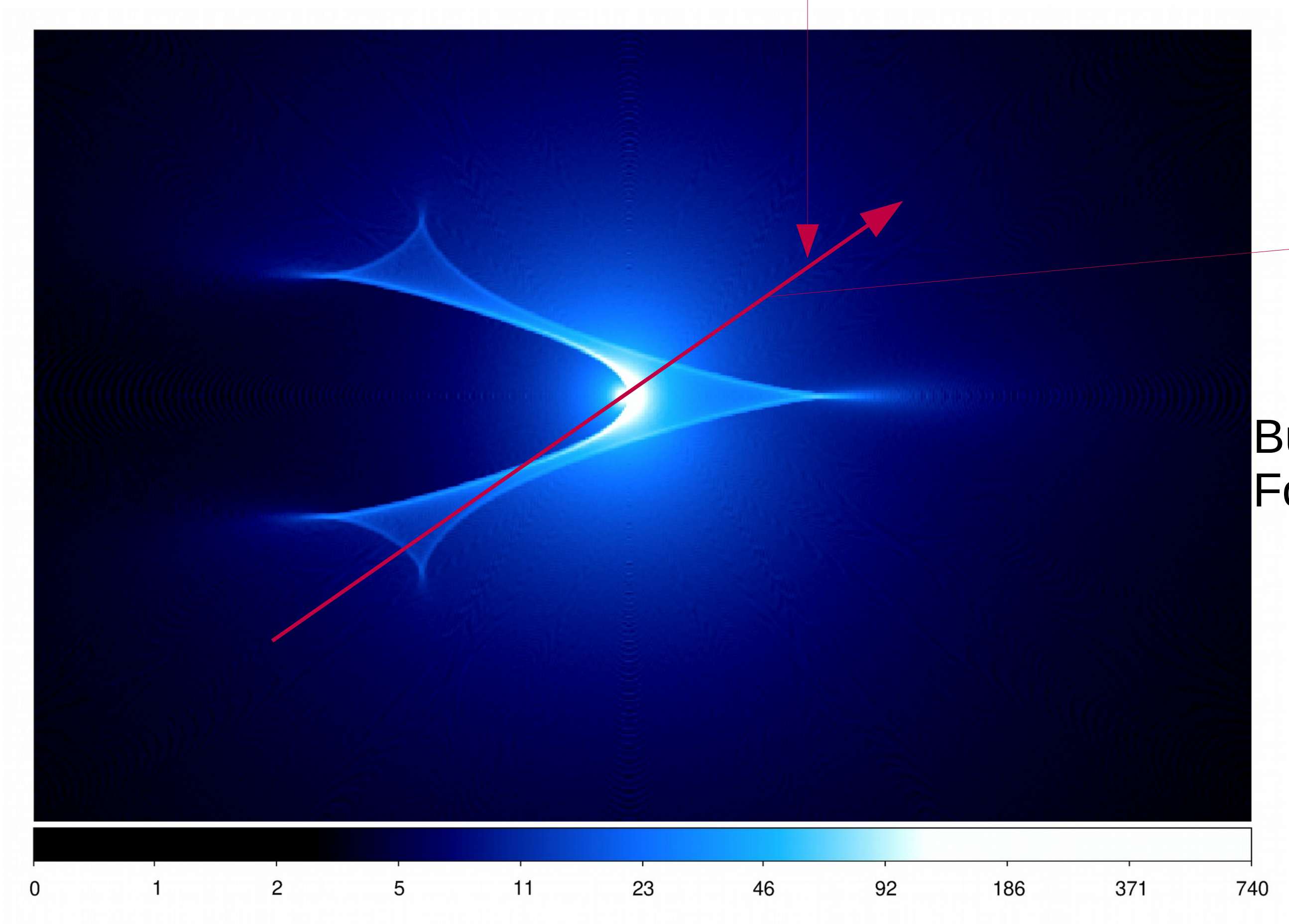

Associated light curve

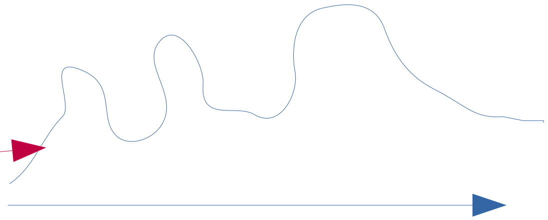

Build a library of light curves
For different distances and mass ratio

Mao & Paczynski (1991)

OGLE-2005-BLG-71

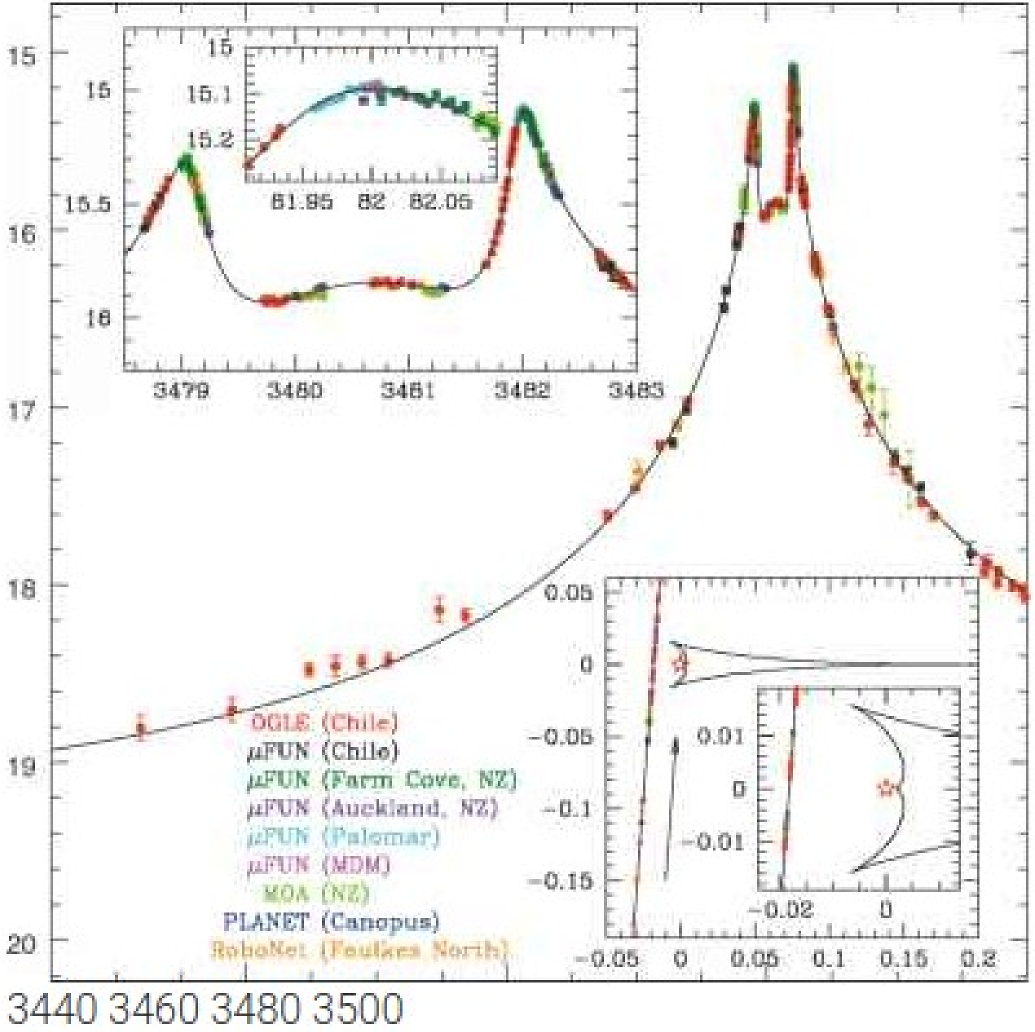

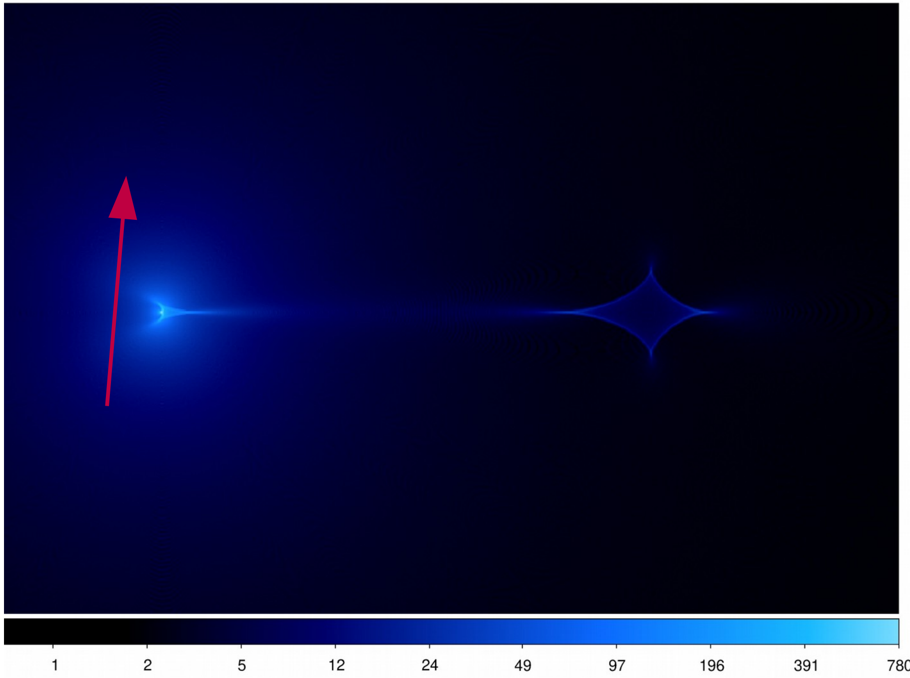

Udalski et al., (2005)

Jovian mass planet

OGLE-2005-BLG-390

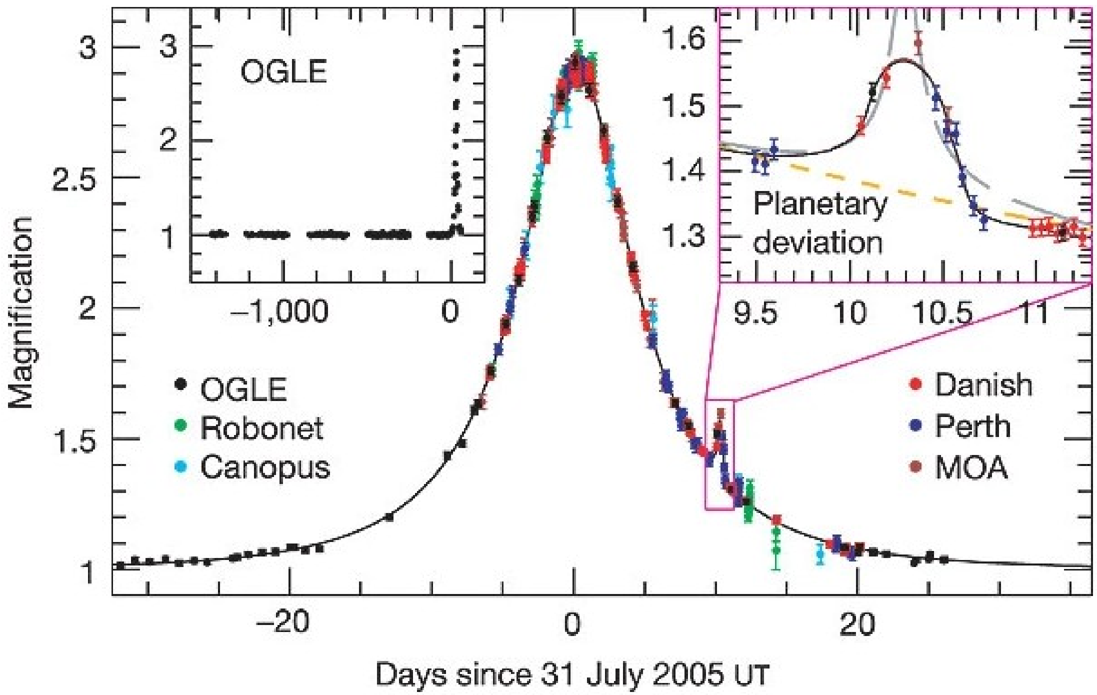

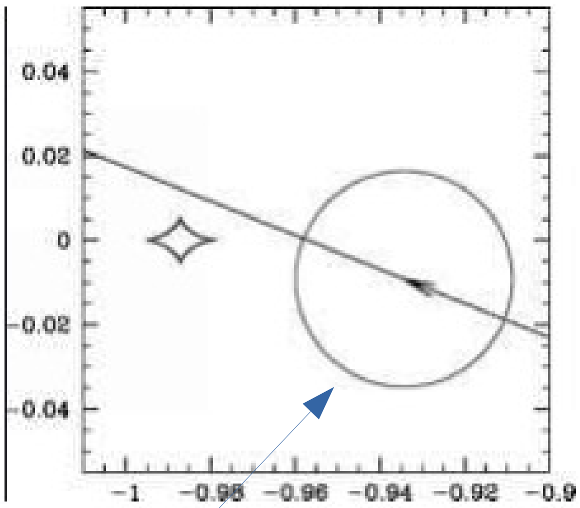

5.5 earth mass planet
cool planet ~ 50 K

Source size is large with respect to caustics

Situation on a global amplification map

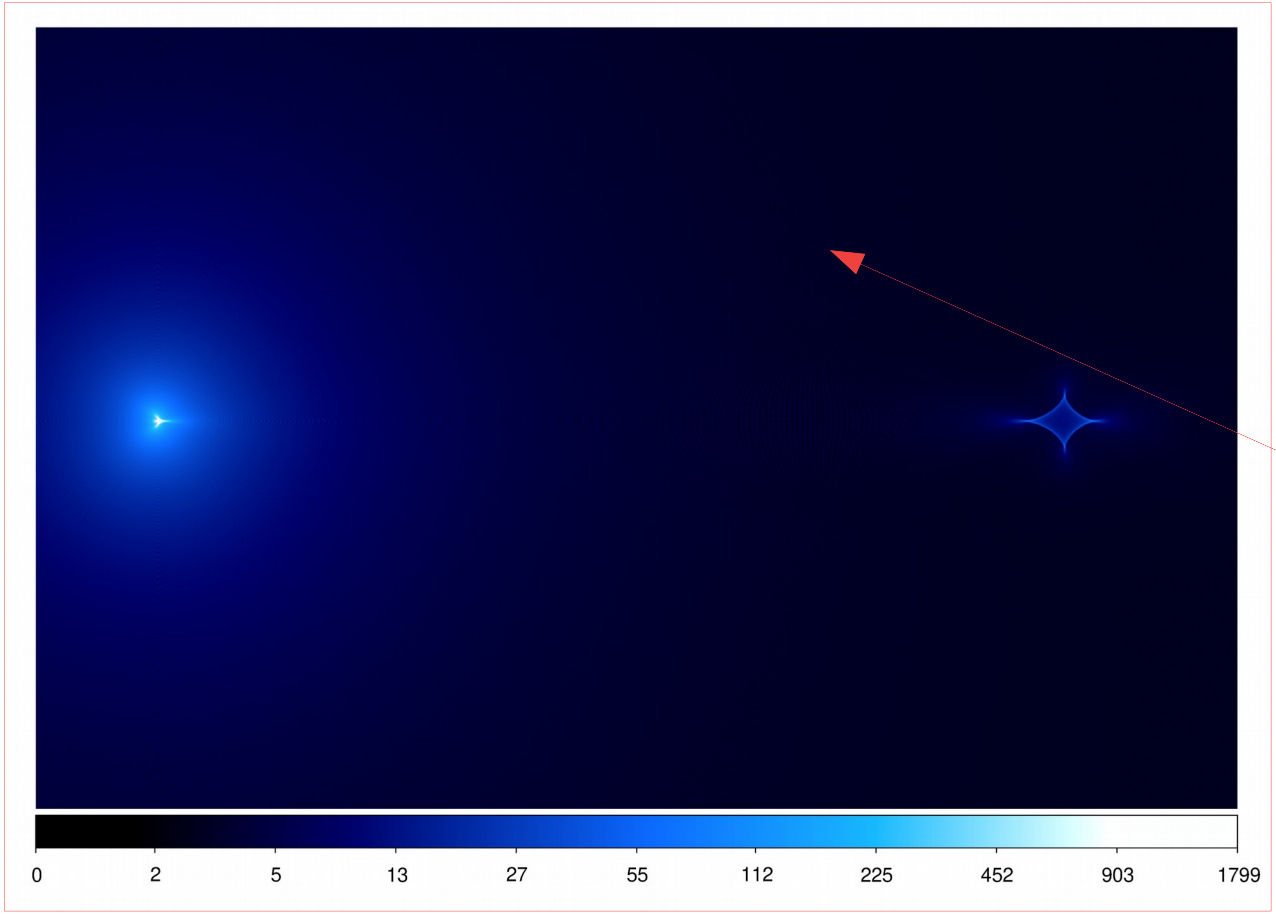

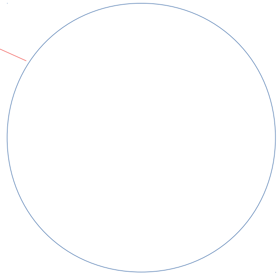

Source size

Detecting planets by microlensing offers important advantages

Not biased to our local environment: planets can be found at few Kpc from us.

Also quite unbiased to short period systems

Very efficient to find planet in the habitability zone around ~ 1 AU

This technique has the best potential to evaluate the statistics of planets in the galaxy

The extrasolar planets discovered

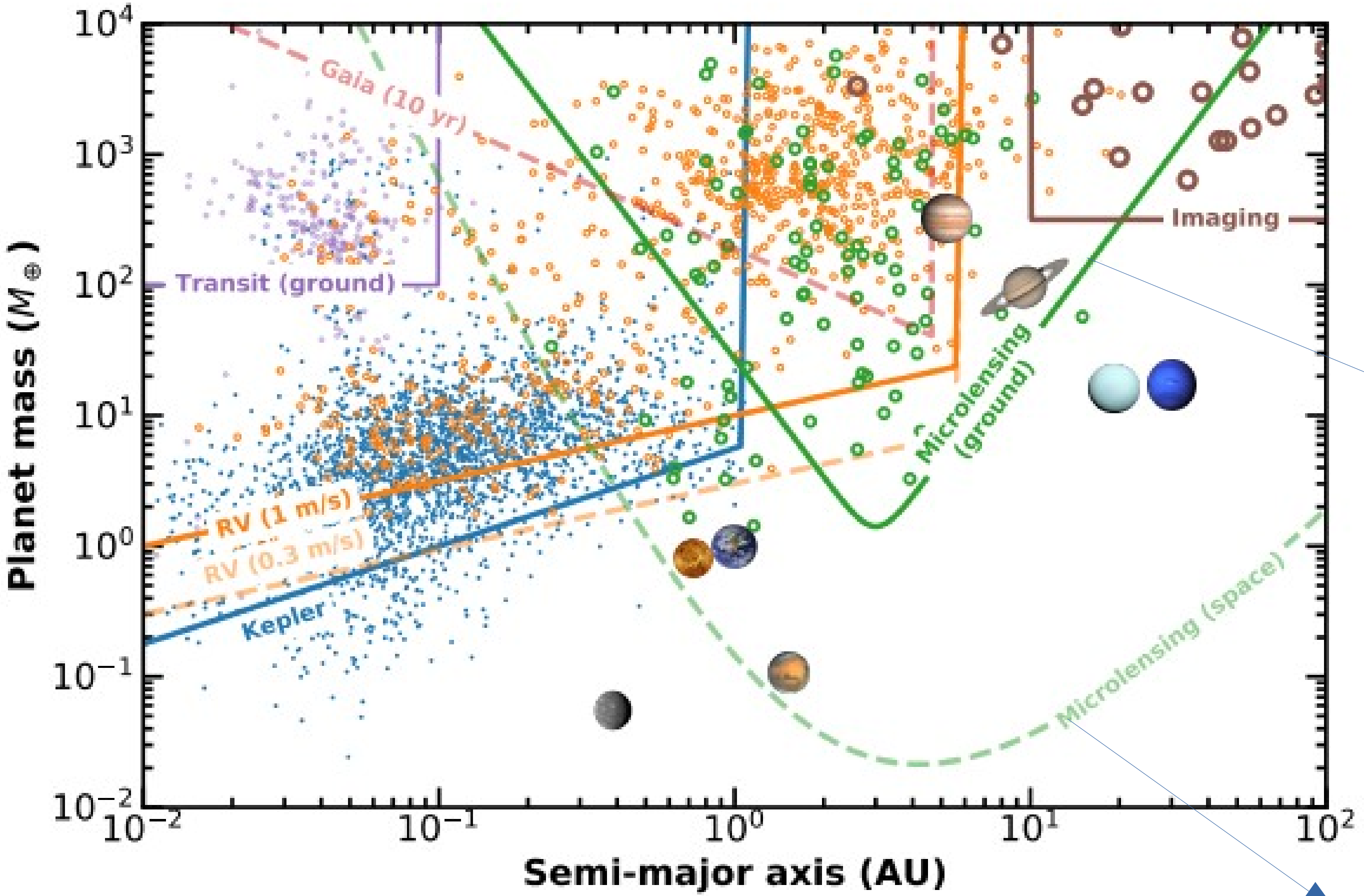

Ground telescopes

WFIRST

Wei & Dong (2021)

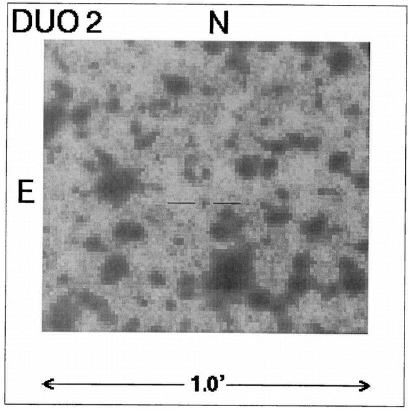

One the first double lens (DUO 2)
(a double system of comparable mass)

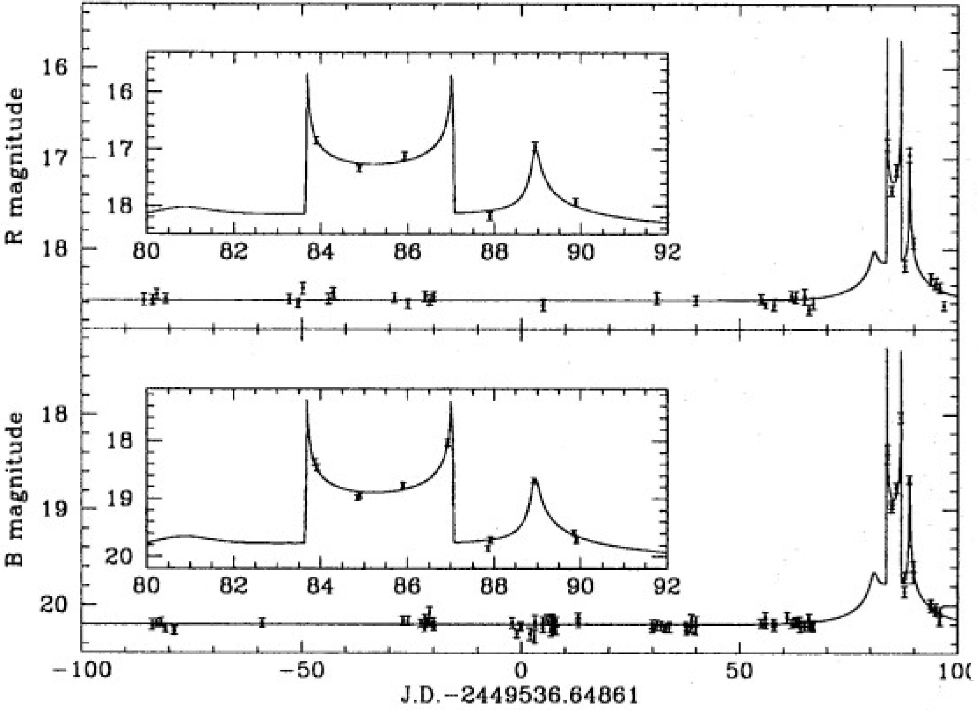

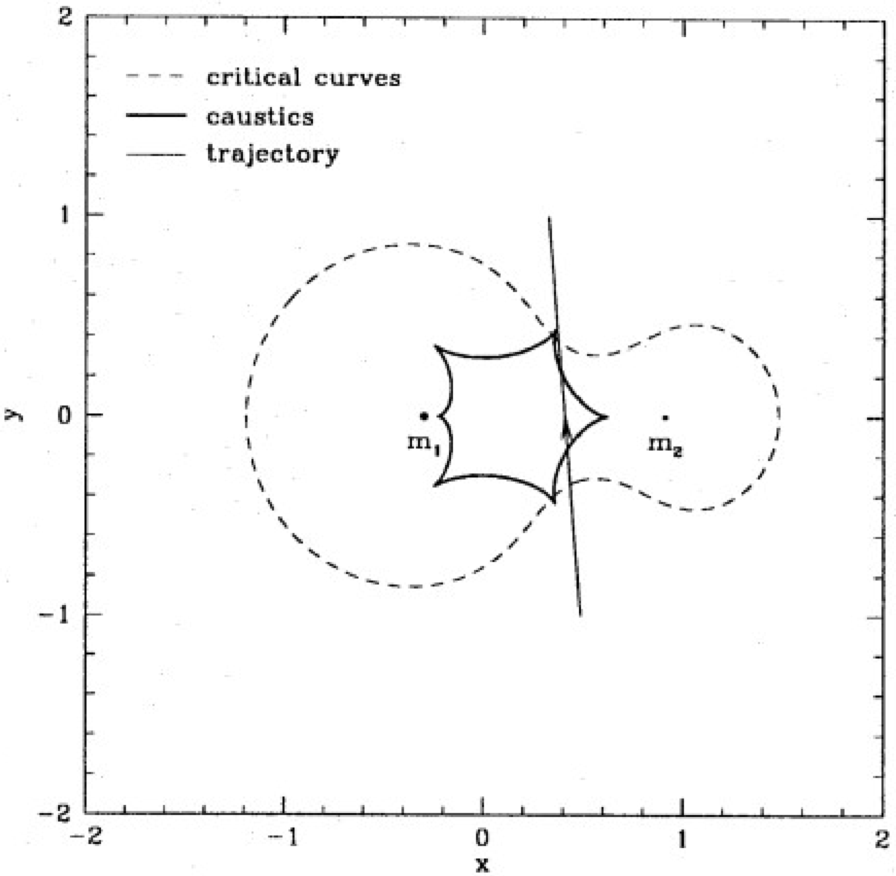

Triple lens system (Han etal. 2012)

Two Jupiter like planet orbiting near the Einstein ring of a solar mass star

HAN ET AL.

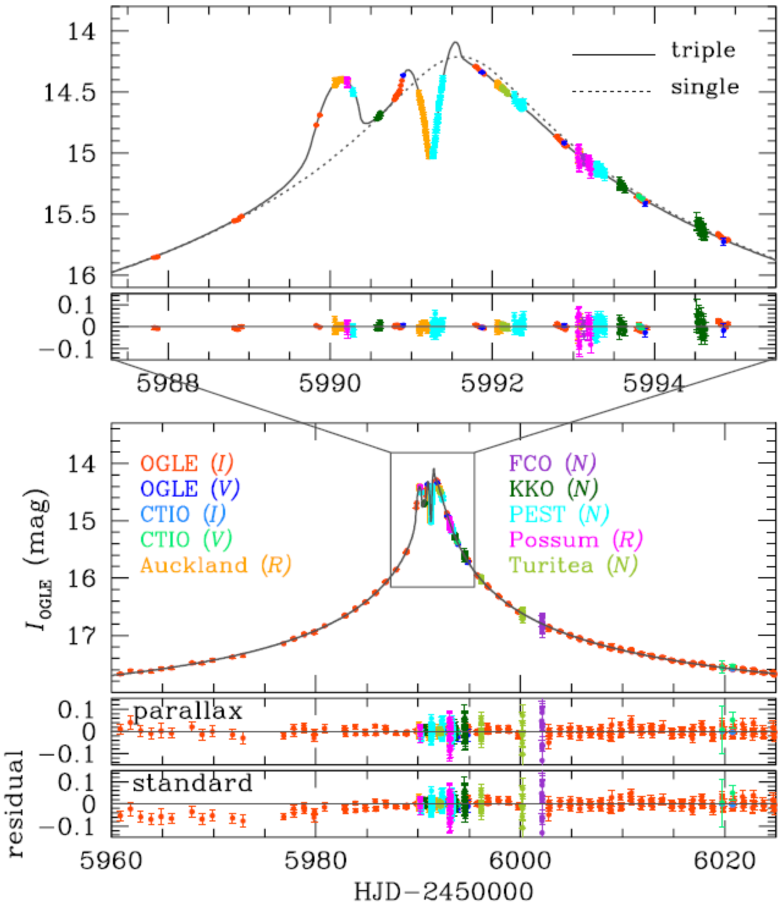

Parallax has been Measured
Distances are known

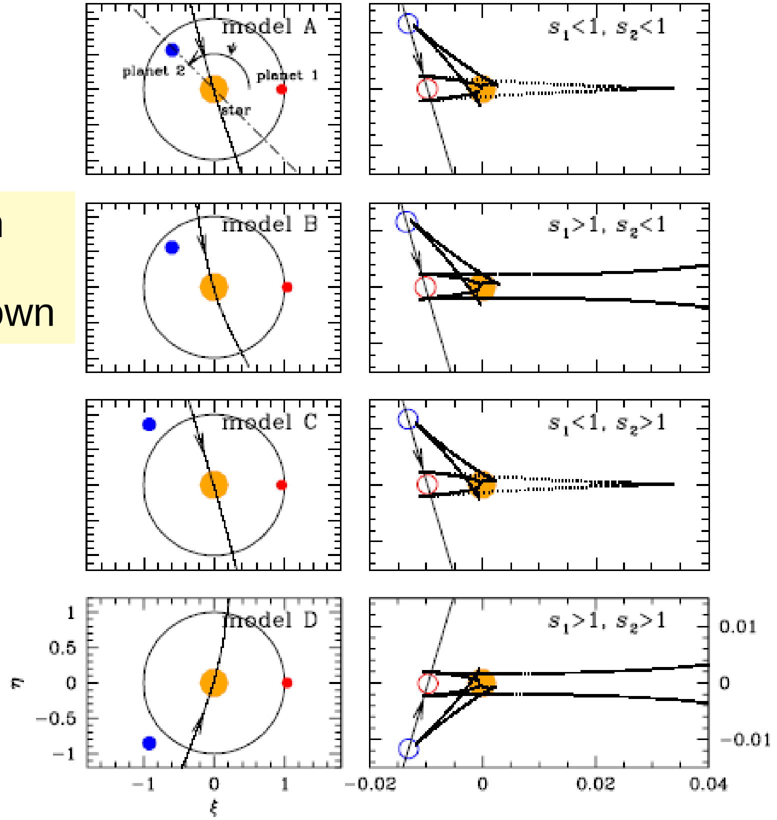

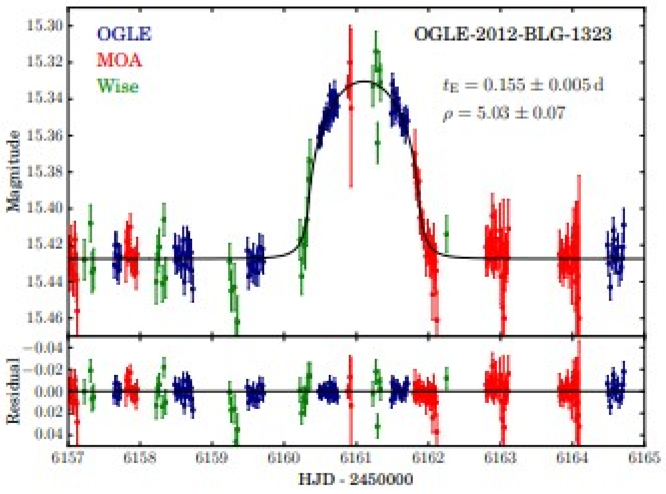

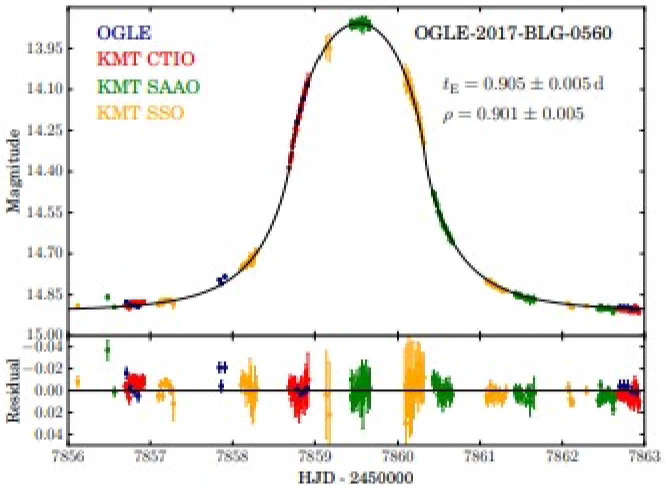

Free floating planets

Planet formation theories predict the ejection of planets

Typical crossing time is short
Due to the low mass of an isolated planet
(a few days)

Mroz, P., *etal.* 2019

A&A 622, A201